(2)

REPORT

NASA CR-185186

THE MEASUREMENT, MODELING, AND PREDICTION OF TRACTION FOR ROCKET PROPELLANT 1

By:

Dr. Joseph L. Tevaarwerk
Senior Research Scientist
Battelle

October 1989

Prepared for:

NATIONAL AERONAUTICS AND SPACE ADMINISTRATION
Lewis Research Center
Cleveland, Ohio 44135

Battelle

REPORT DOCUMENTATION PAGE

Form Approved
OMB No. 0704-0188

1. AGENCY USE ONLY (Leave blank)	2. REPORT DATE	3. REPORT TYPE AND DATES COVERED
	Oct. 1989	Final Report

4. TITLE AND SUBTITLE
The Measurement, Modelling, and Prediction of Traction for Rocket Propellant 1

5. FUNDING NUMBERS
Item 0001CJ
Contract No.
DLA-900-83-C-1744

6. AUTHOR(S)
Dr. J.L. Tevaarwerk
Senior Research Scientist

7. PERFORMING ORGANIZATION NAME(S) AND ADDRESS(ES)
Battelle
Metals and Ceramics Information Center
505 King Avenue
Columbus, OH 43201-2693

8. PERFORMING ORGANIZATION REPORT NUMBER
G8558-8701

9. SPONSORING/MONITORING AGENCY NAME(S) AND ADDRESS(ES)
NASA Lewis Research Center
21000 Brookpark Road
Cleveland, OH 44135

10. SPONSORING/MONITORING AGENCY REPORT NUMBER
NASA CR-185186

11. SUPPLEMENTARY NOTES
Project Manager, C. Woods of the Launch Vehicle Technology Branch in the Space Propulsion Division.

12a. DISTRIBUTION/AVAILABILITY STATEMENT
Public

12b. DISTRIBUTION CODE

13. ABSTRACT (Maximum 200 words)

Traction tests were performed on RP1, a common kerosene based rocket propellant. Traction data on this fluid are required for purposes of turbopump bearing design, using codes such as SHABERTH. To obtain the traction data, an existing twin disc machine was used, operating under the side slip mode and using elliptical contacts. The range of test variables were: contact peak Hertz stress from 1.0 to 2.0 GPa, disc surface speed from 10 to 50 m/s, fluid inlet temperature from 30 to 70 °C, and with a contact aspect ratio of 1.7.

The resulting traction curves were reduced to fundamental fluid property parameters using the Johnson and Tevaarwerk traction model. Theoretical traction predictions were performed by back substitution of the fundamental properties into the traction model. Comparison of the predicted with the measured curves gives a high degree of confidence in the correctness of the traction model. For purposes of input to the NASA SHABERTH program, the traction model was next used to predict the expected traction of RP1 under line contact conditions.

14. SUBJECT TERMS
Traction, Bearings, Rocket Propellant 1, Kerosene, Prediction Measurement, Concentrated Contact Friction

15. NUMBER OF PAGES
VII + 63 pp

16. PRICE CODE

17. SECURITY CLASSIFICATION OF REPORT	18. SECURITY CLASSIFICATION OF THIS PAGE	19. SECURITY CLASSIFICATION OF ABSTRACT	20. LIMITATION OF ABSTRACT
Unclassified	Unclassified	Unclassified	UL

NASA CR-185186

FINAL REPORT

on

THE MEASUREMENT, MODELING, AND PREDICTION OF TRACTION FOR ROCKET PROPELLANT 1

(Item 0001 CJ, Contract No. DLA 900-83-C-1744)

to

NASA LEWIS RESEARCH CENTER

October 26, 1989

By

Dr. J. L. Tevaarwerk

Metals and Ceramics Information Center
A DoD Information Analysis Center

Battelle
. . . Putting Technology To Work

505 King Avenue
Columbus, Ohio 43201-2693

ABSTRACT

Traction tests were performed on RP1, a common kerosene based rocket propellant. Traction data on this fluid are required for purposes of turbopump bearing design, using codes such as SHABERTH. To obtain the traction data, an existing twin disc machine was used, operating under the side slip mode and using elliptical contacts. The range of test variables were: contact peak Hertz stress from 1.0 to 2.0 GPa, disc surface speed from 10 to 50 m/s, fluid inlet temperature from 30 to 70 °C, and with a contact aspect ratio of 1.7.

The resulting traction curves were reduced to fundamental fluid property parameters using the Johnson and Tevaarwerk traction model. Theoretical traction predictions were performed by back substitution of the fundamental properties into the traction model. Comparison of the predicted with the measured curves gives a high degree of confidence in the correctness of the traction model. For purposes of input to the NASA SHABERTH program, the traction model was next used to predict the expected traction of RP1 under line contact conditions.

TABLE OF CONTENTS

TABLE OF CONTENTS (Cont).

NOMENCLATURE

Below follows a list of symbols used in the text and their units.

Symbol	DESCRIPTION	Units
a,b	Semi Hertzian contact size in the x and y direction	[m]
A	Fluid viscosity temperature parameter	[°C]
B	Fluid viscosity pressure parameter	[°C/Pa]
C_s	Specific heat of the disc material	[J/kg.°C]
C	Shear stress temperature constant	[°C/Pa]
C1,2	Number of counter pulses	[-]
D_p	Pressure solidification temperature	[°C]
D_v	Viscosity solidification temperature	[°C]
D_s	Shear stress solidification temperature	[°C]
De	Deborah number	[-]
E	Viscosity constant for non-linear thermal model	[Pa.s]
E'	Composite elastic modulus for the disc material	[Pa]
$E_\emptyset$	Experimental traction viscosity constant	[Pa.s]
E_2	Experimental time delay constant	[-]
F()	Dissipative function for traction model	[s^{-1}]
F_s	Dimensionless thermal resistance of the film	[-]
F_x	Contact force in the x direction	[N]
F_y	Contact force in the y direction	[N]
F_z	Normal force on the contact	[N]
G	Fluid shear modulus (uncorrected)	[Pa]
G_c	Compliance corrected fluid shear modulus	[Pa]
G_e	Johnson's elasticity parameter	[-]
G_s	Shear modulus of the disc material	[Pa]
h	Central film thickness in contact	[m]
J1	Dimensionless longitudinal slip variable	[-]
J4	Dimensionless longitudinal traction variable	[-]
$J4_e$	Elastic stress portion of J4	[-]
$J4_p$	Plastic stress portion of J4	[-]
$J4_t$	Thermal dimensionless longitudinal traction	[-]
k	Contact aspect ratio (b/a)	[-]
k_f	Thermal conductivity of fluid	[W/m °C]
k_s	Thermal conductivity of disc material	[W/m °C]
k'	Fluid thermal conductivity constant	[W/m °C]
k''	Fluid thermal conductivity constant	[°C]
K	Calibration constant in side slip measurement	[m]
m	Initial slope of fluid traction curve	[-]
m'	Initial slope of dry traction curve	[-]
p	pressure	[Pa]
P	Mean Hertz contact pressure	[Pa]
P_o	Hertzian peak contact pressure	[Pa]
P_e	Psuedo Peclet number	[-]
P_r	Reduced Hertz pressure	[Pa]
Q	Kalker coefficient	[-]
R_e	Equivalent radius of curvature for discs	[m]

S	Auxiliary variable used in elastic/plastic model	[-]
s	Roller slip	[-]
t	Time	[s]
U	Rolling speed	[m/s]
ΔU	Slip velocity in x direction	[m/s]
V_o	Viscosity constant	[Pa.s]
ΔV	Side slip velocity of the discs	[m/s]
Δx	Small displacement of the displacement transducer	[m]
YI	Inlet shear heating factor	[-]

GREEK SYMBOLS

β	Side slip angle	[rad]
θ	Temperature of the fluid	[°C]
θ_c	Shearplane temperature	[°C]
θ_o	Inlet or blank temperature	[°C]
Φ	Time delay parameter	[-]
ρ_s	Density of the disc material	[kg/m^{-3}]
χ ψ	Hertzian contact shape parameters	[-]
τ	Fluid shear stress	[Pa]
τ_s	Non linear shear stress parameter	[Pa]
τ_c	Limiting shear strength of fluid	[Pa]
τ_o	Limiting shear strength at inlet temperature	[Pa]
$\dot{\gamma}$	Shear strain rate	[1/s]
μ	Peak traction coefficient	[Pa.s]
η	Viscosity of fluid in the contact	[Pa.s]
η_o	Viscosity constant	[Pa.s]

LIST OF FIGURES

LIST OF TABLES

FINAL REPORT

on

THE MEASUREMENT, MODELING, AND PREDICTION OF TRACTION FOR ROCKET PROPELLANT 1

to

NASA LEWIS RESEARCH CENTER

October 26, 1989

BY

DR. J.L. TEVAARWERK

BATTELLE
505 KING AVENUE

COLUMBUS, OHIO 43201

1-0 INTRODUCTION

Traction or friction plays a major role in today's technological society in that it holds one of the keys to reduce our overall energy consumption, and thereby the dependence on unreliable sources of this energy. Friction and traction indicate the resistance to relative motion of two 'contacting' bodies. The term traction and friction have the same meaning in a tribological sense, however friction is used when this resistance is undesirable and traction is used when it is desirable. The mechanical components in which friction and traction are important are rolling element bearings, gears, cam and tappets, and traction drives. Because these devices almost always operate in a wet or fluid lubricated environment, the traction or friction is mostly governed by the particular fluid that is used. In the first three devices friction is the key source of inefficiency and because of the multitude of bearings and gears in service, a small reduction in these

losses can amount to phenomenal savings in energy. Rolling element bearings actually have rather interesting requirements for friction or traction in that at low to medium speeds friction should be low, but at high speeds traction should be high to ensure that the rolling elements operate at the correct velocities.

In most mechanical devices where friction or traction plays an important role, the lubricating fluid is chosen to optimize the energy efficiency of the device, however, this is not possible in all cases. For example, the bearings used in rocket motor turbopumps are lubricated with the process liquid, may this be a mineral-based low-viscosity fuel such as RP1, or a cryogenic substance such as liquid oxygen or hydrogen. For applications such as these it is critically important that the rheological properties of the working fluid be known and modeled such that a good deal of confidence exists about using the data beyond the range of observation. The data thus obtained can then be used in bearing design codes such as SHABERTH to design for adequate bearing performance for a given mission.

1-1 Prior Traction Investigations

There has been a lot of activity in the area of traction research, both in the past and recently. Notable contributions have come from Clark et al [1951], Smith [1965], Smith et al [1973], Johnson and Cameron [1967], Niemann and Stoessel [1971], and more recently Johnson and Roberts [1974], and Johnson and Tevaarwerk [1977]. Some of these investigations were strictly experimental in nature and aimed at obtaining traction design data, while others were aimed at understanding the traction phenomena so that rheological models could be formulated. This latter research is of course ultimately aimed at relating fluid molecular properties to traction properties. Research by Johnson and Tevaarwerk [1977], Daniels [1978], Hirst and Moore [1980], and Alsaad et al [1978] is directed more towards this purpose. The reader is referred to an excellent review by Johnson, [1978] for further aspects of this topic.

Current understanding of traction has led to traction models that describe the fluid shear behavior in terms of an elastic and a dissipative element. For purposes of mathematical tractability this dissipative element is taken to be plastic like in nature. This gives an adequate description of

the fluid behavior at conditions such as those encountered in rolling element bearings. This work has now been further expanded by developing a simple method to correct for thermal effects due to spin, Tevaarwerk [1981], and an overall thermal traction study, Tevaarwerk [1980].

As with all models, however, their usefulness is severely restricted if inadequate input data is available to the designer. This is especially so if fluids are used that are not normally desirable from a lubrication point of view, but are selected on the basis of other features. RP1 is such a fluid. Being a rocket propellant, based on a high viscosity kerosene, it does not have the traction data base that other more lubricous fluids have. Therefore, it was decided to test its traction behavior experimentally and to use existing rheological models to predict its traction under conditions different from those in the experiments.

The investigation reported herein was performed by Battelle Memorial Institute, of Columbus, Ohio, under contract to the NASA Lewis Research Center through the Metals and Ceramics Information Center, a DOD "Information Analysis Center", Item 0001CJ, Control No. DLA 900-83-C-1744. The NASA technical project manager was C. Woods of the Launch Vehicle Technology Branch in the Space Propulsion Division.

2-0 EXPERIMENTS

The various traction experiments were carried out on an existing twin disc test facility, shown in Figures 2-1, 2-2 and 2-3. The test facility was also used for the traction test results as reported in Tevaarwerk [1983] and [1985]. Traction curves are obtained by using the side slip technique so that large traction transfer can be measured without the need for a large motor/generator set. It also has the advantage that the effects of bearing friction and rolling traction can be corrected for by the simple measurement of the longitudinal slip. This is particularly important when the expected levels of fluid friction are low, as is the case with the lubricant tested here. With longitudinal traction measurements the correction for bearing friction and rolling traction is often of the same magnitude as the measured traction with these lubricants.

2-1 Description of Twin Disc Machine.

For an extensive description of twin disc traction testers the reader is referred to the literature; Smith [1965] and Johnson and Roberts [1974]. Basically the machine consists of two discs, called the toroid (upper) and disc (lower). The lower disc is mounted in rolling element bearings through shafts and the only degree of freedom is one of rotation about this axis. The lower disc always has a transverse radius of curvature of infinity. The upper disc is contained in bearings that are mounted in the upper assembly. This upper assembly is suspended with elastic hinges such that only direct normal motion and axial motion is possible. The assembly will however always stay horizontal. The toroid (or upper) has curvatures to produce the desired contact geometry is arrived at. The upper assembly is constructed such that the toroidal axis can be tilted relative to the horizontal plane so as to introduce spin on the contact. It can also be skewed about the normal to the contact to introduce a side slip velocity.

In order to achieve the range of pressures required for the traction data, a set of discs with a nominal aspect ratio of 1.7 is used. These discs are made of AISI-01 steel, hardened to 7.00 GPa, ground and polished to a surface finish of less than .05 μm RMS and with an out-of-roundness error of less than 5 μm. Between tests the discs are inspected for surface damage and,

if needed, reground and polished to bring them back up to specifications. The required normal load, obtained by a dead loading technique, can be calculated from the Hertz theory for elastic bodies in contact. The maximum contact normal stress P_o is given by:

$$P_o = \frac{1}{2\pi\psi\chi}^{3} \frac{3F_z E'^2}{R_e^2} \quad , \tag{2-1}$$

where,

F_z	= contact normal load,	[N]
P_o	= Hertzian contact stress,	[Pa]
E'	= composite elastic modulus, (231 GPa for steel)	[Pa]
R_e	= equivalent disc radius,	[m]
	= $(1/R_x + 1/R_y)^{-1}$, and	
ψ, χ	= Hertzian contact shape factors.	[-]

2-2 Instrumentation of the Traction Tester

By suitably instrumenting the disc machine the relevant experimental parameters can be measured. In the experiments reported here the sideslip, sideways traction force, disc surface temperature, rolling velocity, and the amount of longitudinal slip are measured. The technique of measuring each of these variables will be discussed next.

2-2-1 The Measurement of the Traction Force

A ring dynamometer type load cell is used to measure the side slip force of the upper toroid assembly. The electrical signal from the load cell is conditioned for noise and amplified using common mode rejection techniques. The gain on the amplifier is adjusted so that a good range on the signal is measured for each test. Calibration of the load cell is done in situ by dead loading. This calibration is checked periodically.

2-2-2 The Measurement of Side Slip

The skew angle is measured by using a direct current displacement transducer on the upper assembly and thereby measuring the rotation angle of this assembly. This skew angle gives the amount of side slip/roll ratio through the relationship:

(2-2) $$\Delta v/U = \tan(\beta) \ ,$$

where,

β = side slip angle, [rad]
Δv = side slip velocity, and [m/s]
U = rolling velocity. [m/s]

By measuring the amount of skew with the displacement transducer the side slip/roll ratio is obtained directly through:

(2-3) $$\Delta v/U = K\Delta x \ .$$

where Δx is the displacement of the transducer and K a scale factor. The electrical output of the displacement transducer is filtered in an R-C network to provide a low-pass signal. The maximum frequency response of the R-C network is 0.1 s. The displacement transducer is calibrated by rotating the upper assembly through a known angle and then calculating the amount of side slip for this angle.

2-2-3 The Measurement of Rolling Velocity and Longitudinal Slip

The rotational velocities of both the disc and the toroid are measured by using a MC 6840 frequency counter. The proximity probes for the control of the counters are mounted near the support bearings, see Fig. 2-3. Each shaft has a simple protrusion on it that produces a pulse once per revolution. This pulse is used to turn countdown counters on when controlled to do so. The next successive pulse from the proximity probe stops the countdown. When each of the two counters has completed its cycle, a flag is set and the register contents are read. From the difference between the original and the final

contents of the registers, the amount of time for a single revolution of each shaft is calculated. From this the angular speed for each shaft is determined, and hence the peripheral velocity of each roller can be calculated if the roller radius is known. The countdown frequency on the counters is selected such that an accuracy of at least 1: 10000 is obtained. By employing this method the slip of the rollers can be measured every five or six revolutions of the shafts. From the countdown and the undeformed roller radii the slip is calculated as follows:

$$(2\text{-}4) \qquad s = 2\,\frac{U2 - U1}{U2 + U1} = 2\left(\frac{R2}{R1} - \frac{C2}{C1}\right) \Big/ \left(\frac{R2}{R1} + \frac{C2}{C1}\right) [-] \ .$$

This can be approximated if the amount of slip is small by the following:

$$(2\text{-}5) \qquad s \overset{\sim}{=} \left(\frac{R2}{R1} - \frac{C2}{C1}\right),$$

where,

s	= roller slip,	[-]
U	= rolling velocity,	[m/s]
C	= number of count down pulses, and	[-]
R	= roller radius.	[m]

Suffix 1 denotes the toroid and suffix 2 denotes the disc. It should be stressed that the actual amount of slip will be somewhat different when two different roller materials are in contact because of the deformation of the rollers themselves. The errors thus introduced can be removed by measuring the rolling slip at very low rolling speeds.

2-2-4 The Measurement of the Disc Surface Temperature

In the analysis and reduction of the test data it is important that the disc temperature be used as the reference inlet temperature for the film thickness. This temperature can be measured by embedding a thermocouple directly below the surface of the disc and then to take this signal out through slip rings. This method is however not very practical when a number of different discs are involved and is also very costly from an installation point of view. With care the surface temperature can also be measured by

using a trailing thermocouple that rides on the disc surface. The disadvantage of this technique is that it can be speed sensitive in its response because of frictional heating.

The latter technique is employed here and care is taken to ensure that the contact force on the thermocouple is not excessive. A temperature reference bath junction ensures that the same reference level for the thermocouple is used at all times. The signal from the thermocouple is amplified using common mode rejection techniques to minimize the influence of electrical noise and other disturbances. Calibration is done by the boiling water method adjusted for sea level differences. This calibration is checked periodically. Only slight deviations are encountered. Because of the frictional heating at the junction/toroid interface a variation of about 2 C° is found in the signal between stationary discs and those rotating at a surface velocity of 120 m/s. The overall reproducibility of the temperature measurement is better than 2 C°.

The temperature on the machine is regulated through the use of heaters and coolers on the test fluid. This test fluid is allowed to circulate freely before the start of a test series in order to bring the machine up to a uniform temperature. No specific effort is made however to maintain a given set point temperature during the test and the reason for this will become clear in the analysis of the results.

2-3 Traction Measurements

Traction curves are obtained by the slow rotation of the upper assembly from a positive value of side slip/roll ratio to a negative value. The signals from the above discussed transducers are fed into a digitizer from where they are led into a data logging computer for plotting and storage on magnetic media for future use. The computer automatically traces the force versus slip curve on the screen. By reversing the direction of rotation of the machine, a duplicate set of curves can be obtained. For each experiment 500 data points are taken at fixed time periods of 0.2 seconds. Multiple data points are stored as separate entries.

After the completion of a test series the data is recalled into memory of the computer and further manipulated. This manipulation consists of the averaging of the multiple entries, the filling in of any gaps in the data

through forward and backward interpolation, the comparison of the traces for the forward and reverse rolling direction, and the centering of the traces about the center lines. After the centering operation the data is smoothed by a 'N' point averaging technique for traction points after the peak traction points. For storage a geometric series is used so that the total traction trace is now represented by 40 data points for each measured variable. These traces are stored on magnetic media and used for further manipulation and data extraction at a later point.

2-4 Traction Curves For RP1

A survey of the literature revealed that very little traction data is available on low viscosity fluids such as RP1. This is especially so in the higher speed ranges of 10 m/s and above. Hence it was decided to perform traction tests on RP1 over a fairly broad speed, pressure, and temperature range. The nominal test matrix consisted of the following:

Contact Pressure P_o:	1, 1.3, 1.6, and 2.0,	[GPa]
Rolling speed U:	± 10, ± 30, ± 50,	[m/s]
Temperature θ_o:	25 and 75,	[°C]
Slip $\Delta V/U$:	-0.05 to 0.20, and	[-]
Spin $\frac{\omega_1 ab}{U}$:	0.	[-]

This test matrix leads to 24 different traction test curves. The measured value being the traction coefficient F_y/F_z as a function of slip. The traction data measured on RP1 using the equipment and techniques as described above are shown in Appendix I. The lettered labels in each curve are used only for identification purposes and do not indicate an actual measured data point.

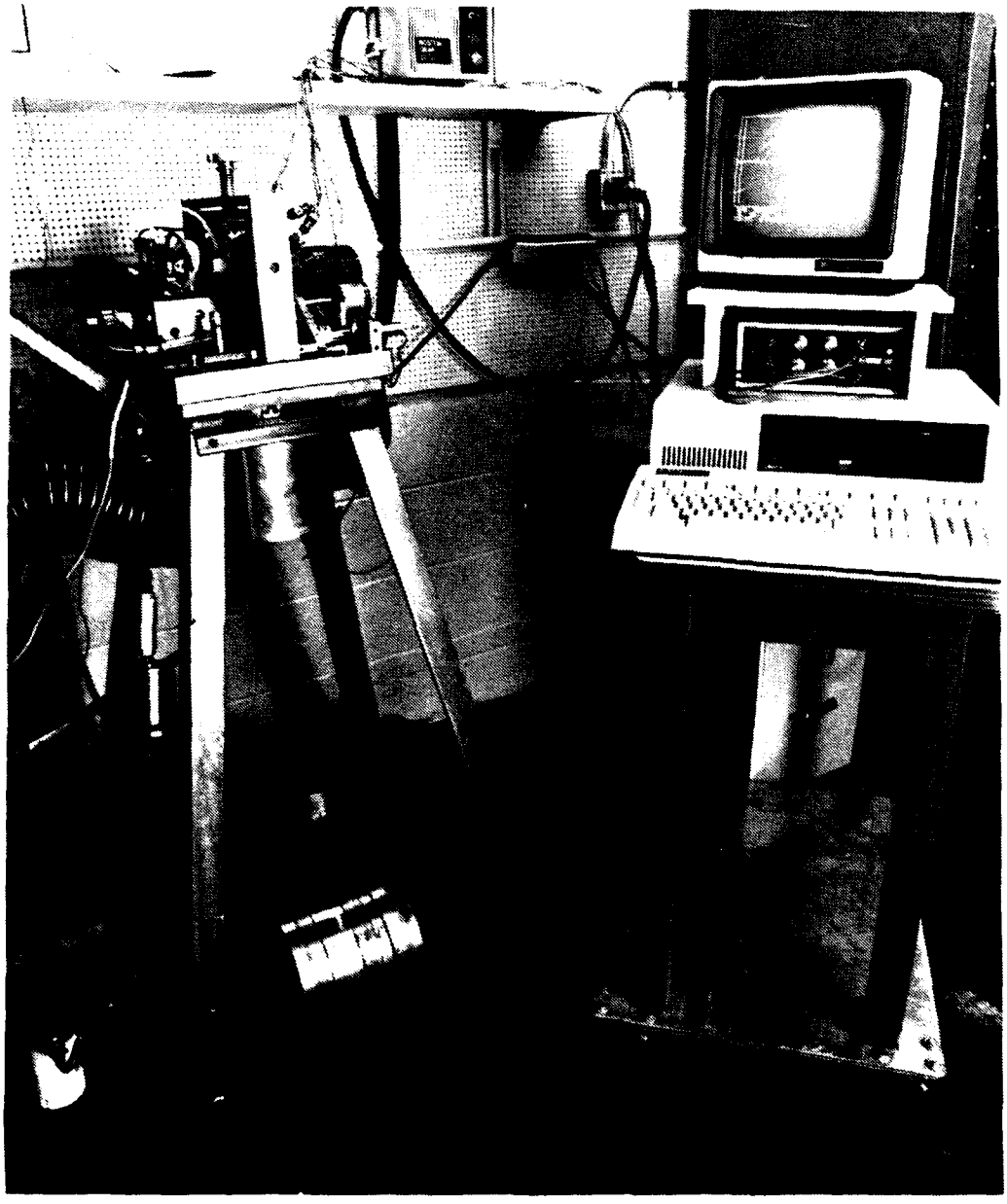

FIGURE 2-1. OVERVIEW OF HIGH PERFORMANCE SIDE SLIP TRACTION TESTER

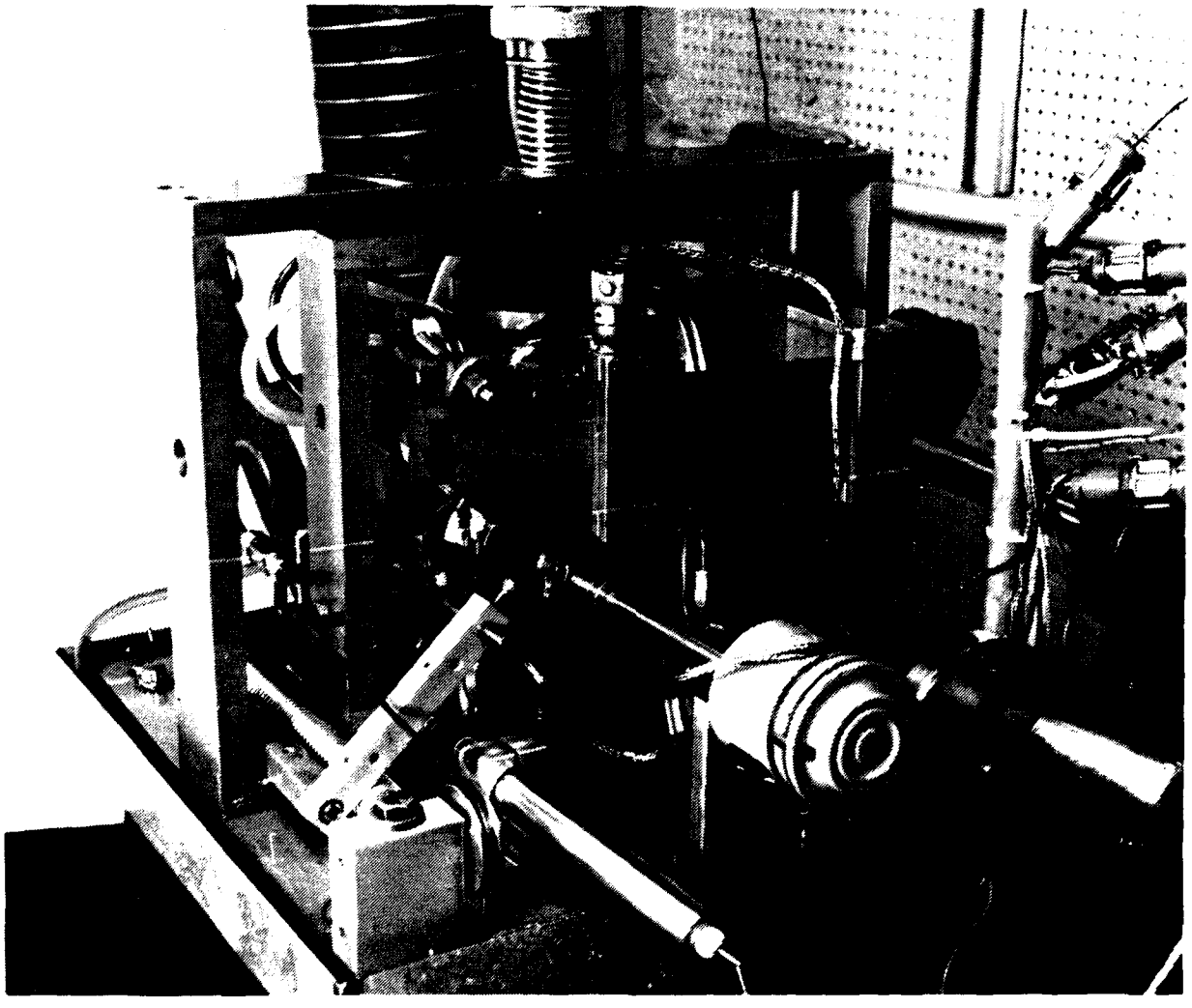

FIGURE 2-2. RIGHT HAND VIEW OF HIGH PERFORMANCE SIDE SLIP TRACTION TESTER

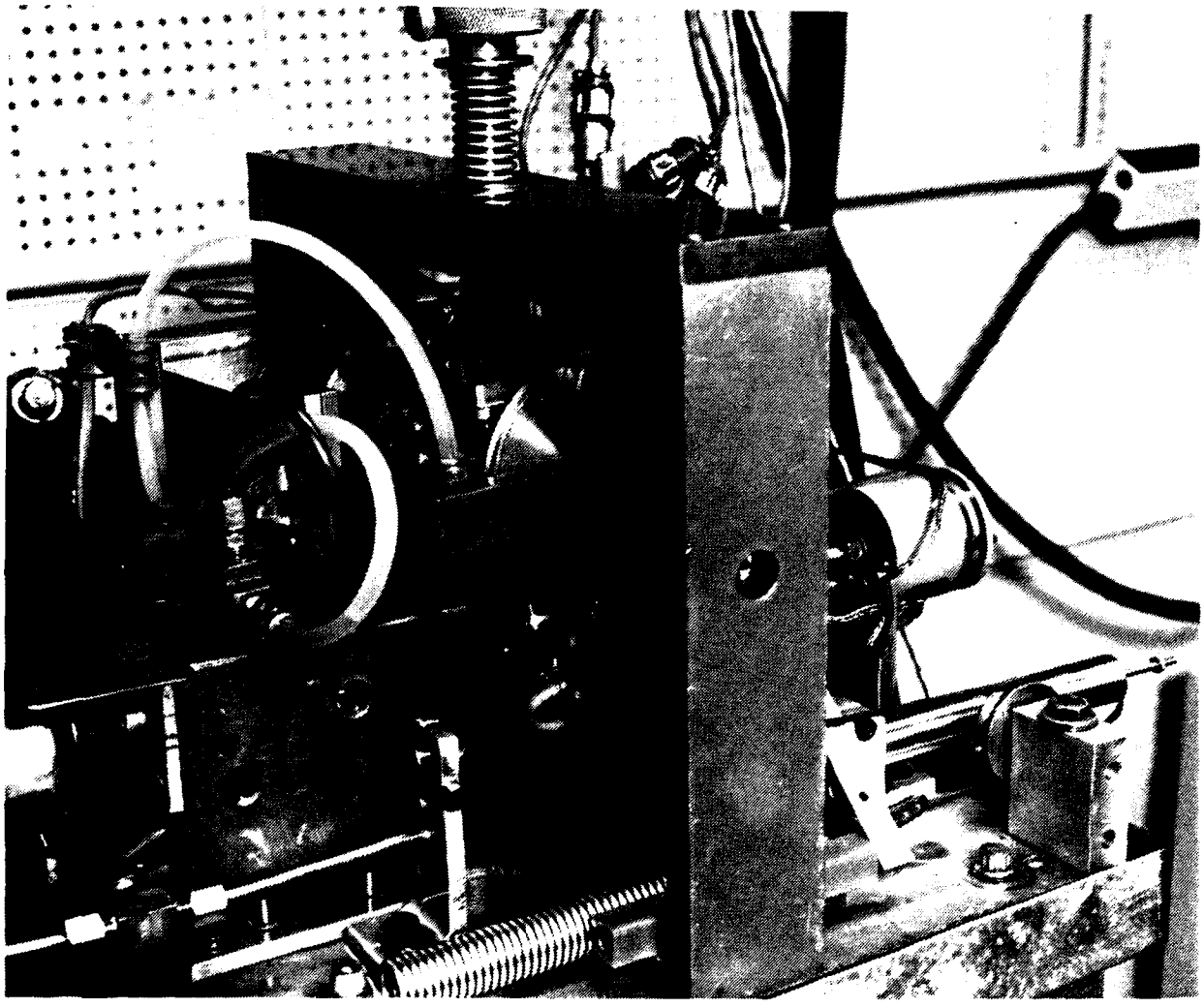

FIGURE 2-3. LEFT HAND VIEW OF HIGH PERFORMANCE SIDE SLIP TRACTION TESTER

3-0 THEORETICAL ANALYSIS

In order to understand the required analysis of the experimental data it will be helpful to consider the following discussion of traction. The ability of a fluid film, trapped under high pressure in the elastically deformed region of two loaded curved elements, to transmit a tangential force from one element to the other is commonly referred to as friction or traction. The magnitude of this force depends on several variables such as :1) the contact kinematic conditions of slip, spin and sideslip, 2) the fluid present, 3) temperature, pressure and operating speeds. We will examine the traction behavior under simple slip only.

Under conditions of increasing slip between the two elements, an increasing traction force is transmitted up to a certain limit at which point it will decrease with further slip. See Figure 3-1.

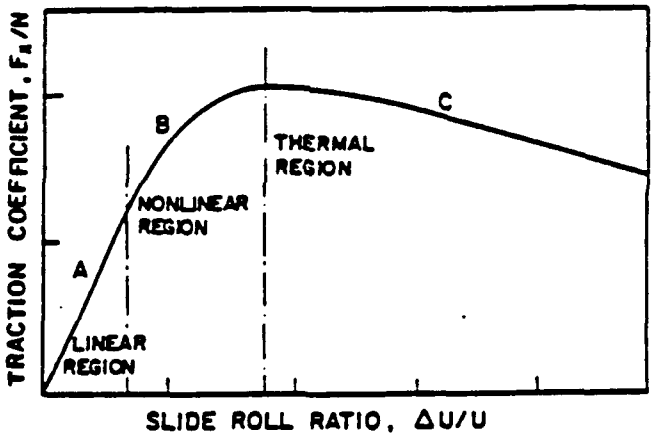

FIGURE 3-1. TYPICAL TRACTION /SLIP CURVE

There are three regions identified on this traction curve and the behavior in each of these regions can best be described by the Deborah number (De). For a simple Maxwell viscoelastic model this number is the ratio of the relaxation time and the mean transit time, see Johnson and Tevaarwerk, [1977].

(A) The linear low slip region. Thought to be isothermal in nature, it is caused by the shearing of a linear viscous fluid (low De) or that of a linear elastic solid (high De).

(B) The nonlinear region. Still isothermal in nature but now the viscous

element responds nonlinearly. At low De this portion of the traction curve can be described by a suitable nonlinear viscous function alone, while at high De a linear elastic element interacts with the nonlinear viscous element.

(C) At yet higher values of slip the traction decreases with increasing slip and it is no longer possible to ignore the dissipative shearing and the heat that it generates in the film. Johnson and Cameron [1967] showed that the shear plane hypothesis advanced by Smith [1965] does account for most of their experimental observations in this region. More recently Conry et al [1979] have shown that a nonlinear viscous element together with a simple thermal correction can also describe this region.

3-1 Isothermal Traction Analysis

The rheological model that describes the traction under simple slip in all three regions of operation fairly well is the J & T traction model as presented by Johnson and Tevaarwerk [1977]:

$$\frac{1}{G}\frac{d\tau}{dt} + F(\tau) = \dot{\gamma} \quad , \tag{3-1}$$

where,

τ	= shear stress,	[Pa]
G	= shear modulus,	[Pa]
t	= time, and	[s]
$\dot{\gamma}$	= shear strain rate.	[1/s]

The dissipative function $F(\tau)$ is open to the choice of the researcher to fit the observed traction, but Johnson and Tevaarwerk [1977] found that the hyperbolic sine:

$$F(\tau) = \frac{\tau_s}{\eta} \sinh\left(\frac{\tau}{\tau_s}\right) \quad , \tag{3-2}$$

where,

τ_s = non-linear shear stress parameter. [Pa],
η = local viscosity [Pa.s],

described all of their experimental results in regions (A) and (B) very well.

At higher pressures and for fluids with high traction coefficients this dissipative function may be replaced by the purely plastic behavior of the material:

$$(3\text{-}3) \qquad F(\tau) = 0 \text{ for } \tau < \tau_c \; ; \; F(\tau) = \dot{\gamma}^{\circ} \text{ for } \tau = \tau_c \; ,$$

where,

τ_c = limiting shear strength of the fluid [Pa].

Whether the perfectly plastic behavior of the material is intrinsic is not clear. Work by Johnson and Greenwood [1980] suggests that it is possibly the result of thermal behavior of the sinh model. For many applications the elastic/plastic traction model is adequate. It was used by Tevaarwerk and Johnson [1979c] and Tevaarwerk [1979b] to predict traction under various conditions of slip and spin. The analysis is completely isothermal in nature and for simple slip the traction is given by:

$$(3\text{-}4) \qquad J4 = \frac{2}{\pi} \left[\tan^{-1} S + \frac{S}{(1 + S^2)} \right] \; ,$$

where, $S = \frac{2}{3} \frac{J1}{\sqrt{k}}$, $J1 = \frac{\bar{G}}{\tau_o} \frac{\sqrt{ab}}{h} \frac{\Delta U}{U}$, and $J4 = \frac{F_x}{\mu F_z}$.

The shear strain rate in the fluid was taken to be the same everywhere in the contact and assumed to be constant throughout the film thickness. Its magnitude was taken to be:

$$\dot{\gamma}^{\circ} = \frac{\Delta U}{h} \; .$$

Equation (3-4) results from the integration of stresses caused by the shearing of an elastic element of pressure-independent average-shear-modulus G and the plastic stresses proportional to the local Hertzian pressure. The predicted traction from an elastic/plastic model compares very well with the experimentally observed values for combinations of slip and spin, provided that the spin or slip are not too large. Large slip or spin results in almost

purely dissipative stresses over the contact area and hence non-isothermal behavior. Traction prediction under these conditions is still possible but the thermal effects need to be brought into the picture. Tevaarwerk [1981a], [1979c] presents two techniques for calculating such spin traction curves. The former technique requires the shape of the traction curve in the large slip regime to provide a simple correction to the isothermally predicted spin traction.

3-2 Thermal Traction Analysis

The ability to separate the elastic stresses from the plastic ones can be used to perform a thermal traction calculation. The analysis presented here follows the technique outlined by Tevaarwerk [1980] and [1983].

Equation (3-4) resulted from the integration of isothermal elastic and plastic stresses over the contact area of an ellipse. For the region of contact under elastic stress, the shear energy is conserved and therefore does not give rise to temperature increases. The plastically deforming region, however, is non-conservative and a temperature rise in the fluid is expected. This will lead to a reduction in the local strength of the fluid. Equation (3-4) may therefore be better written in its elastic and plastic parts:

$$J4 = J4_p + J4_e \quad , \tag{3-5}$$

$$J4_e = \frac{4\,S}{\pi(1+S^2)^2} \quad , \text{ and} \tag{3-6}$$

$$J4_p = \frac{2}{\pi}\left[\tan^{-1}S + \frac{S(S^2-1)}{(1+S^2)^2}\right] \quad . \tag{3-7}$$

Equation (3-5) may now be modified by τ_c/τ_o where τ_c is the average stress under thermal conditions and τ_o is the average stress under isothermal conditions. We are dealing therefore with averaged stresses in the plastic region of the contact even though the isothermal stress distribution is according to the Hertzian pressure. This seemingly contradictory

assumption is supported by theoretical evidence by Tevaarwerk [1979c]. The modified equation would therefore be:

$$(3\text{-}8) \qquad J4_t = J4_e + \frac{\tau_c}{\tau_o} J4_p \quad .$$

The modification term τ_c/τ_o can be found from a thermal balance over the contact region under plastic stress. This region can be thought of as a thermal source whose heat is conducted/convected away. The length of the source is a function of the location of the onset of plastic deformation after the initial elastic region, however in this simple model we will take the source length to be "a" where this is the semi contact length in the running direction. As a simple thermal balance we will use the expression reported by Johnson and Cameron [1967] for the shear plane temperature:

$$(3\text{-}9) \qquad \theta_c - \theta_o = q \frac{h}{k_f} \left[F_s + \frac{.5}{\sqrt{P_e}} \right] \quad ,$$

where,

$$(3\text{-}10) \qquad P_e = \frac{a \rho_s C_s U}{k_s} \left\{ \frac{k_s\ h}{k_f\ a} \right\}^2 \quad , \qquad [-]$$

and,

q	= average thermal strength of the source,	[W/m^2]
θ_c	= shearplane temperature in the contact,	[°C]
θ_o	= inlet temperature of the fluid,	[°C]
k_f	= thermal conductivity of fluid in the contact,	[W/m°C]
h	= central film thickness in the contact,	[m]
k_s	= thermal conductivity of the roller material,	[W/m°C]
C_s	= specific heat of the roller material,	[J/kg°C]
ρ_s	= density of the roller material, and	[kg/m^3]
F_s	= thermal resistance of the film.	[-]

This expression is valid only when the heat is conducted through the film and convected away by the discs, a condition that is true for most concentrated contacts. The strength q of the source is given by:

(3-11) $$q = \tau \Delta U \ .$$

The thermal resistance of the film F_s may be found by calculating the average film temperatures due to distributed sources and is normally taken to be:

(3-12) $$F_s = 0.1.$$

In order to proceed any further we need a relationship between temperature and the shear strength of the fluid. A typical relationship that has its roots in the Eyring theory of fluid transport is given by:

(3-13) $$\tau(\theta) = \frac{1}{C} \left[A + BP + (\theta+D) \ \mathrm{Ln} \left(\frac{2 \ CE\dot{\gamma}^{\circ}}{\theta+D} \right) \right] \ ,$$

where,

A	= viscosity temperature constant,	[°C]
B	= pressure viscosity constant,	[°C/Pa]
C	= non-linear shear stress constant,	[°C/Pa]
D	= fluid solidification temperature,	[°C]
E	= fluid viscosity, and	[Pa.s]
P	= pressure of the fluid in the contact.	[Pa]

At first sight it seems that this equation has five disposable constants in it. However, two of these constants (A and D) may be obtained from the atmospheric viscosity temperature relationship, and one more (B) can be obtained from the Barus viscosity pressure relationship. The constant D is known as the solidification temperature, the temperature to which the fluid should be cooled to become solid like under atmospheric pressure. Only the constants C and E need to be determined experimentally from the traction results and this will be done in the next chapter. It should be noted here that the ultimate aim is to derive the fluid traction parameters such that they apply for all the experimental conditions reported here.

By using equations (3-9), (3-10), (3-11), and (3-13) the average thermal shear stress can be obtained for a given set of conditions. In equation (3-8) we need the ratio of the average contact shear stress under thermal conditions to that under isothermal conditions. This is really the ratio of the shear stress given by equation (3-13) evaluated at the shearplane temperature θ_c (from equation 3-9) and the shear stress as evaluated at the inlet temperature

conditions θ_o. The other contact conditions remain the same for this ratio calculation.

The method that is outlined above was used for the traction data analysis as reported by Tevaarwerk [1985]. For the analysis of the traction data as reported here, several improvements were made in the model and these changes are outlined in the next chapter.

4-0 EXTRACTION OF THE TRACTION PARAMETERS

In order to use the traction model to calculate the level of traction in a given contact condition, the relevant traction parameters need to be extracted. In equation (3-1) we saw that both the elastic effects and the nonlinear viscous effect account for the behavior of the fluid. Elastic effects are typically felt under conditions of high contact pressure, low temperature, and high speed.

4-1 Extraction of The Shear Modulus Parameters

As discussed in chapter 3 the initial linear slope on a traction curve can be the result of either a viscous or an elastic response of the material in the contact to the strain implied. The parameter that determines the actual response is the dimensionless grouping of the relaxation time of the material in the contact and the transit time of this material through the contact. For a simple Maxwell type material this number is known as the Deborah number and is given by:

$$De = \frac{\eta U}{aG} , \tag{4-1}$$

where,

η	=	viscosity of the fluid in the contact,	[Pa.s]
U	=	transit velocity of fluid in the contact,	[m/s]
a	=	semi contact length in rolling direction, and	[m]
G	=	shear modulus of the fluid in the contact.	[Pa]

Under the assumptions of a simple pressure distribution according to Hertz, a constant film thickness in the contact, and a constant shear modulus over the contact area, the initial small strain behavior for the material will be elastic if the Deborah number is larger than 10 and will be viscous in response if the Deborah number is less than 0.1. In between these two values the response is due to a mixed viscoelastic behavior.

Many assumptions have been made before arriving at this point, however even with more complicated analyses where the pressure is allowed to influence

the viscous and elastic properties it is found that the transition points occur at about the same Deborah numbers. Also for the range of parameters normally encountered in traction contacts the Deborah number is such that the initial slope of the traction curve is almost always governed by the elastic properties of the contacting material. In the analysis of the data as performed here this assumption is implicit.

4-1-1 Shear Modulus For Constant Properties

When the initial linear response is completely elastic it is quite easy to calculate the value for the actual modulus that caused this slope. Under the assumptions of constant properties throughout the contact this modulus can be extracted from the initial slope using the following equation:

$$G = \pi m \frac{P_o h}{4a} \qquad [Pa]. \tag{4-2}$$

This equation is applicable regardless of whether the slope is measured under longitudinal slip or under side slip. Using the known values of m, P_o, and a, and a calculated value of h for film thickness, it is quite simple to calculate the fluid shear modulus G.

4-1-2 Shear Modulus With a Simple Compliance Correction

One of the criticisms that is often raised at the above analysis is that it neglects the influence of the disk compliance on the measured slope. Disk compliance is the result of the elastic creepage of the disk material due to the tractive stresses on the surface. The traction response in the initial linear range is affected by this disk creepage in that it makes the slopes lower than if the discs were infinitely stiff. An exact correction of the modulus for the disc compliance is not possible at the moment. The analysis that is presented here is that due to Johnson and Roberts [1974].

If we let m' be the slope of the traction curve for dry rolling bodies, then from the addition of the compliances of the discs and the film a simple corrective term for the shear modulus may be derived as shown in

Equation (4-3). From this expression it is obvious that when the measured slope approaches the dry slope the corrected value for the shear modulus tends to infinity.

$$(4\text{-}3) \qquad G_c = G\left(\frac{m'}{(m'-m)}\right) \quad , \qquad [Pa]$$

where G_c = simple compliance corrected modulus.

The dry slope m' can be calculated from the expression given by Kalker [1967] as:

$$(4\text{-}4) \qquad m' = \frac{G_s}{QP_o} \quad , \qquad [-]$$

where,

G_s = shear modulus of the disc material, and [Pa]
Q = Kalker coefficient. [-]

The value of the Kalker coefficient depends on the aspect ratio of the contact and the direction of slip. Below is a table which gives these values for the tests as reported here.

Table 4-1. Kalker Coefficients Q for Sideslip

aspect ratio k	coefficient Q
1	.56
2	.70
5	.81

4-2 Extraction of the Large Strain Parameters

The large slip region , that is the region beyond the traction peak, is almost exclusively governed by the dissipative element in the rheological equation. With the elastic effects becoming insignificant it is now quite easy to extract the governing parameters for this region. In essence what is required is a reverse analysis of the traction calculation normally used for the calculation of the traction curves. When the elastic response of the fluid is no longer dominant, the shear strain rate in the film is taken by the viscous element and we may express equation (3-1) as:

$$(4\text{-}5) \qquad F(\tau) = \dot{\gamma} = \frac{\tau_s}{\eta} \sinh\left(\frac{\tau}{\tau_s}\right) \quad .$$

When the argument τ/τ_s is larger than 1 this may be further simplified to the following:

$$(4\text{-}6) \qquad F(\tau) = \dot{\gamma} = \frac{\tau_s}{2\eta} \operatorname{Exp}\left(\frac{\tau}{\tau_s}\right) .$$

This expression relates the stress to strain response for a small element of fluid that is subjected to a shear strain rate, $\dot{\gamma}$, at a given pressure and a given temperature. Each of the parameters in this equation can be a function of temperature or pressure or both. In the analysis of traction it is normally sufficient to treat the fluid viscosity as a function of temperature and pressure and to make the non-linear stress parameter a function of temperature only. The following relationships will be used here:

--- for the viscosity we will combine the Vogels temperature viscosity and the Barus pressure viscosity relationships as follows:

$$(4\text{-}7) \qquad \eta\ (\theta,\ p) = \eta_o \exp\left(\frac{A}{\theta + D_v} + \frac{pB}{\theta + D_p}\right) , \qquad [Pa.s]$$

where,

η_o	= viscosity constant,	[Pa.s]
A	= temperature viscosity constant,	[°C]
D_v	= solidification constant for Vogels equation,	[°C]
B	= pressure viscosity constant,	[°C/Pa]
D_p	= solidification constant for Barus equation,	[°C]
θ	= local temperature, and	[°C]
p	= local pressure.	[Pa]

-- for the temperature dependence of τ_s on the local temperature we will use the following:

$$\tau_s = \frac{\theta + D_s}{C} \quad , \tag{4-8}$$

where,

C = non linear shear stress constant [°C/Pa], and
D_s = solidification constant for Eyring equation [°C].

These parameters (except for the temperature and the pressure) are all constants for a given fluid.

In order to proceed any further we have to make some assumptions about the conditions within the contact. First, we will assume that average conditions exist for the contact. Hence temperature and pressure are only mean temperatures and pressures. Second, we will assume that the important temperature for the analysis is the shear plane temperature as given by Equation (3-9). Third, the shear strain rate $\dot{\gamma}$ will be assumed to be constant throughout the film and, in the case of the traction experiments, is constant over the contact area. Its magnitude is given by:

$$\dot{\gamma} = \Delta v/h, \text{ and} \quad [s^{-1}] \tag{4-9}$$
$$h = \text{central filmthickness} \quad [m]$$

The central film thickness is calculated from the expressions by Hamrock and Dowson [1977]. Further modifications to this film thickness to allow for inlet shear heating are made by using the Murch and Wilson [1975] approach. Hence in total we will make the following simplifications:

(4-10)

	local	average	equation #
temperature	θ	θ_c	(3-9)
shear strain rate	$\dot{\gamma}$	$\Delta v/h$	(4-9)
pressure	p	$2P_o/3$	(2-1)
shear stress	τ	$F_y/\pi ab$	

By substituting the expressions from equation (4-7) to (4-9) into Equation (4-2) we obtain:

$$\frac{\Delta v}{h} = \frac{\theta_c + D_s}{2CV_o} \quad \text{Exp} \left(\frac{\tau_c C}{\theta_c + D_s} - \frac{A}{\theta_c + D_v} - \frac{B\,P}{\theta_c + D_p} \right). \tag{4-11}$$

At a first glance there appear to be 7 parameters that can be used to fit the data. This is not the case however because several of these are determined by the results from other experiments. For example, the correlation of the viscosity data for the lubricants to equation (4-3) solves for the constants A, B, D_v, and D_p. It remains therefore to find the constants D_s and C. These can be derived from the thermal region of the traction curve itself by curve fitting Equation (4-11) to it. For this purpose it is better to write this equation in a slightly different form:

$$\frac{\tau_c}{\theta_c + D_s} = \frac{1}{C} \left[\frac{A}{\theta_c + D_v} + \frac{BP}{\theta_c + D_p} + \text{Ln} \left(\frac{2CV_o\ \Delta v}{(\theta_c + D_s)\ h} \right) \right]. \tag{4-12}$$

From the above equation it is apparent that if this relationship holds then the results from the traction measurements should form a straight line when plotted in the above fashion. The slope of this line gives the value for C while the value of D_s can be calculated by adjusting it until the best fit is obtained.

4-3 Reduced Pressure Effects

When a fluid film is present in the contact zone the pressure distribution is not strictly Hertzian but modified by the fluid. Due to the hydrodynamic action the pressure distribution is more peaky, and is spread over a broader area. This will lead to a reduction in the mean pressure in the contact. The reduced pressure may be calculated from the pressure ratio as given below:

$$P_r = P\,[1 - 4\,G_e^{-0.25}\,YI^{-3}\,e^{(-2.3/k)}]\ , \tag{4-13}$$

where,

G_e	= Johnson's elasticity constant,	[-]
P	= mean Hertz contact pressure,	[Pa]
YI	= Inlet shear heating factor,	[-]
k	= aspect ratio (b/a),	[-]
P_r	= reduced contact pressure,	[Pa]

4-4 Transit Time Dependence

The fluid in the contact is subjected to very high pressure gradients for a very short time duration. It is therefore not likely that the viscosity in the contact has reached equilibrium conditions. How near equilibrium that it is will depend on several factors such as the time it is subjected to the pressure and the ease with which the molecules can rearrange themselves. A suitable dimensionless grouping that takes these various factors into account is given as:

$$\Phi = \frac{U\,\eta(\theta_o)}{a\,P_o}\ , \tag{4-14}$$

where,

Φ	= dimensionless time delay parameter,	[-]
U	= mean roller speed,	[m/s]
$\eta(\theta_o)$	= viscosity at inlet temperature,	[Pa.s]
a	= semi Hertz contact length, and	[m]
P_o	= Hertz contact pressure.	[Pa]

This parameter is used in conjunction with the viscosity constant in the following way:

$$V_o = E_o \Phi^{E2}, \qquad [Pa.s] \tag{4-15}$$

where,

E_o = equilibrium viscosity, and [Pa.s]
E_2 = time delay exponent. [-]

The single constant V_o has now been replaced by this two constants equation so we have increased our degree of freedom by one for the system.

4-5 Thermal Conductivity Temperature Dependence

It may be expected that the thermal conductivity of the fluid is a function of the temperature. This has a direct influence on the thermal resistance of the fluid in the contact. In order to take this effect into account the thermal conductivity is fitted to the following equation:

$$k_f = \frac{k'}{\theta_c + k''} \quad . \qquad [W/m\ °C] \tag{4-16}$$

Since the shear plane temperature occurs in equation (4-12) and the thermal conductivity occurs in equation (3-9), the solution to both the thermal conductivity and the shear plane temperature must be done on an iterative basis.

4-6 Determination of the Experimental Parameters

We are now in a position to use the data obtained from the traction experiments and fit the rheological model to them. As stated earlier, the viscosity temperature-pressure data for the traction data reduction may be obtained from isobaric and isothermal viscosity measurements. Similarly the thermal conductivity data can be obtained from published information on RP1 in the Liquid Propellant Manual [1982]. The following sections will deal with

the determination of the actual numerical values of the various constants needed for the equations of state and the constants needed for the fluid rheology.

4-6-1 Determination of Viscosity Temperature Pressure and Temperature Conductivity Parameters

Not all of the constants in Equation (4-12) need to be determined from the experimental traction data. The temperature viscosity characterization may be used to solve for A and D_v while the pressure viscosity effects can be used to solve for B and D_p.

The viscosity temperature data may be obtained from the Liquid Propellant Manual [1982]. Pressure viscosity data for RP1 was taken from the data generated by Bridgeman [1970] for kerosene. Using these two sources of information allows the determination of the constants in Equation (4-7).

(4-7) $$\eta\ (\theta,\ p) = \eta_o \exp\left(\frac{A}{\theta + D_v} + \frac{pB}{\theta + D_p}\right) , \qquad [Pa.s]$$

where,

$A = 542.4$,	[°C]
$B = 544$,	[GPa^{-1}]
$D_v = 143$,	[°C]
$D_p = 25.6$, and	[°C]
$\eta_o = 6.33 \times 10^{-5}$	[Pa.s]

Thermal conductivity data for RP1 was taken from the Vargaftik [1983]. Fitting this data to Equation (4-16),

(4-16) $$k_f = \frac{k'}{\theta_c + k''} . \qquad [W/m\ °C]$$

results in the following values for k' and k"

$k' = 61.6$, and	[W/m °C]
$k'' = 535.5$	[°C]

4-6-2 Experimental Shear Modulus from Traction Data

Similar to the non-linear stress parameter τ_c, it is found that the fluid shear modulus as extracted from traction tests is influenced by the inlet temperature, by the contact pressure, and by the rolling speed. As a fairly simple relationship the following expression is used:

$$G_c = \frac{G_1 + G_2\, P + G_3\, |U|}{\theta + D_v} \qquad \text{[Gpa]} \tag{4-17}$$

where,

$G_{1,3}$	=	experimental constants,	
P	=	contact pressure,	[GPa]
U	=	rolling velocity, and	[m/s]
D_v	=	Vogels fluid solidification temperature.	[°C]

Using the initial slopes from the traction experiments and some regression analysis the following values were found for the constants $G_{1,3}$.

G_1	=	1.0	[GPa °C]
G_2	=	0.25	[°C]
G_3	=	-0.005	[GPa °C s/m]

To obtain this data, the high pressure, low temperature curves were mostly used in the calculations.

4-6-3 Experimental Traction Constants

By combining the Equations (4-8), (4-9) and (4-10) the large slip traction data may be fitted to the following equation:

$$\frac{\tau_c}{\theta_c + D_s} = \frac{1}{C}\left[\frac{A}{\theta_c + D_v} + \frac{BP}{\theta_c + D_p} + \mathrm{Ln}\left(\frac{2CV_o\,\Delta v}{(\theta_c + D_s)\,h}\right)\right], \tag{4-12}$$

where the shear plane temperature is calculated from equation (3-9) as:

$$(3\text{-}9) \qquad \theta_c - \theta_o = q \frac{h}{k_f} \left[F_s + \frac{.5}{\sqrt{P_e}} \right] .$$

P_e is given by Equation (3-10) as:

$$(3\text{-}10) \qquad P_e = \frac{a \rho_s C_s U}{k_s} \left\{ \frac{k_s \, h}{k_f \, a} \right\}^2 [-] ,$$

and F_s is:

$$(3\text{-}12) \qquad F_s = 0.1$$

The constants that remain to be solved for at this point are:

$$C, \; D_s, \; E_o, \text{ and } E_2.$$

These can now be solved for by using a successive regression analysis on the large slip traction data. This was performed using the experimental traction data as reported in Chapter 2. A summary of the test data used and the calculated values for some of the intermediate parameters are shown in Table 4-2. The thermal properties for the test disc material was taken to be:

$$(4\text{-}18) \qquad \begin{array}{ll} k_s = 15, & [W/m \; °C] \\ C_s = 500. & [J/kg \; °C] \end{array}$$

The degree of fit obtained from the data on Equation (4-12) is shown in Figure 4-1. From this regression analysis the following constants resulted:

$$(4\text{-}19) \qquad \begin{array}{lll} C = 2.75 \times 10^{-5}, & & [°C/Pa] \\ D_s = 143, & & [°C] \\ E_o = 6.96 \times 10^{-5}, \text{ and} & & [Pa.s] \\ E_2 = -0.057. & & [-] \end{array}$$

TABLE 4-2. TRACTION CURVE DATA ANALYSIS FOR RP1

The following oil properties were used in the analysis:
Viscosity temperature: A= 542.4 'C D=143.0 'C V0= .0000633 Pas
Viscosity Pressure : B= 544.0 'C/GPa Dp= 25.6 'C
Thermal Conductivity : K'= 535.5 W/m'C K''= 61.7 'C
Eyring Dpress= 25.6 : Peak Factor= .98
Disc Thermal Conductivity : Ks= 15 W/m'C Specific Heat=500 J/kg'C

****

TEST INCLUDED IN THE MULTIPLE TRACTION DATA ANALYSIS

Test # (----)	Po (GPa)	Uo (m/s)	To ('C)	Fz (N)	kk (-)	a (mm)	Pes (-)	Tshear ('C)	H0 mic	Yi --	Plot Mark
RP196M1TR	1.01	10.3	34	200	1.7	.235	2	47	.097	.98	A
RP196M2TR	1.01	30.4	35	200	1.7	.235	26	61	.193	.92	B
RP196M3TR	1.01	49.6	39	200	1.7	.235	65	71	.237	.87	C
RP196M4TR	1.27	11.5	37	400	1.7	.297	2	61	.093	.98	D
RP196M5TR	1.27	30.8	38	400	1.7	.297	18	76	.175	.92	E
RP196M6TR	1.27	50.0	41	400	1.7	.297	44	92	.211	.87	F
RP196M7TR	1.60	11.9	39	800	1.7	.374	1	75	.086	.98	G
RP196M8TR	1.60	30.5	40	800	1.7	.374	11	99	.150	.93	H
RP196M9TR	1.60	50.5	44	800	1.7	.374	31	117	.188	.88	I
RP196MATR	1.92	11.8	40	1380	1.7	.448	1	91	.077	.98	J
RP196MBTR	1.92	31.4	44	1380	1.7	.448	7	119	.128	.94	K
RP196MCTR	1.92	50.0	49	1380	1.7	.448	19	141	.157	.89	L
RP196N1TR	1.01	49.5	58	200	1.7	.235	37	84	.175	.90	M
RP196N2TR	1.01	30.7	57	200	1.7	.235	13	74	.135	.94	N
RP196N5TR	1.27	30.9	60	400	1.7	.297	9	87	.123	.94	O
RP196N6TR	1.27	50.0	62	400	1.7	.297	26	97	.158	.90	P
RP196N7TR	1.60	50.5	64	800	1.7	.374	19	122	.146	.90	Q
RP196N8TR	1.60	31.9	64	800	1.7	.374	6	108	.110	.94	R
RP196N9TR	1.60	11.3	64	800	1.7	.374	0	91	.054	.99	S
RP196NATR	1.92	11.2	64	1380	1.7	.448	1	107	.057	.98	T
RP196NBTR	1.92	31.1	66	1380	1.7	.448	4	127	.097	.95	U
RP196NCTR	1.92	49.6	69	1380	1.7	.448	12	142	.127	.91	V
RP196NETR	1.01	30.5	64	200	1.7	.235	11	79	.122	.94	W
RP196NGTR	1.27	51.0	63	400	1.7	.297	26	99	.159	.90	X
RP196NHTR	1.27	30.6	61	400	1.7	.297	9	89	.121	.94	Y

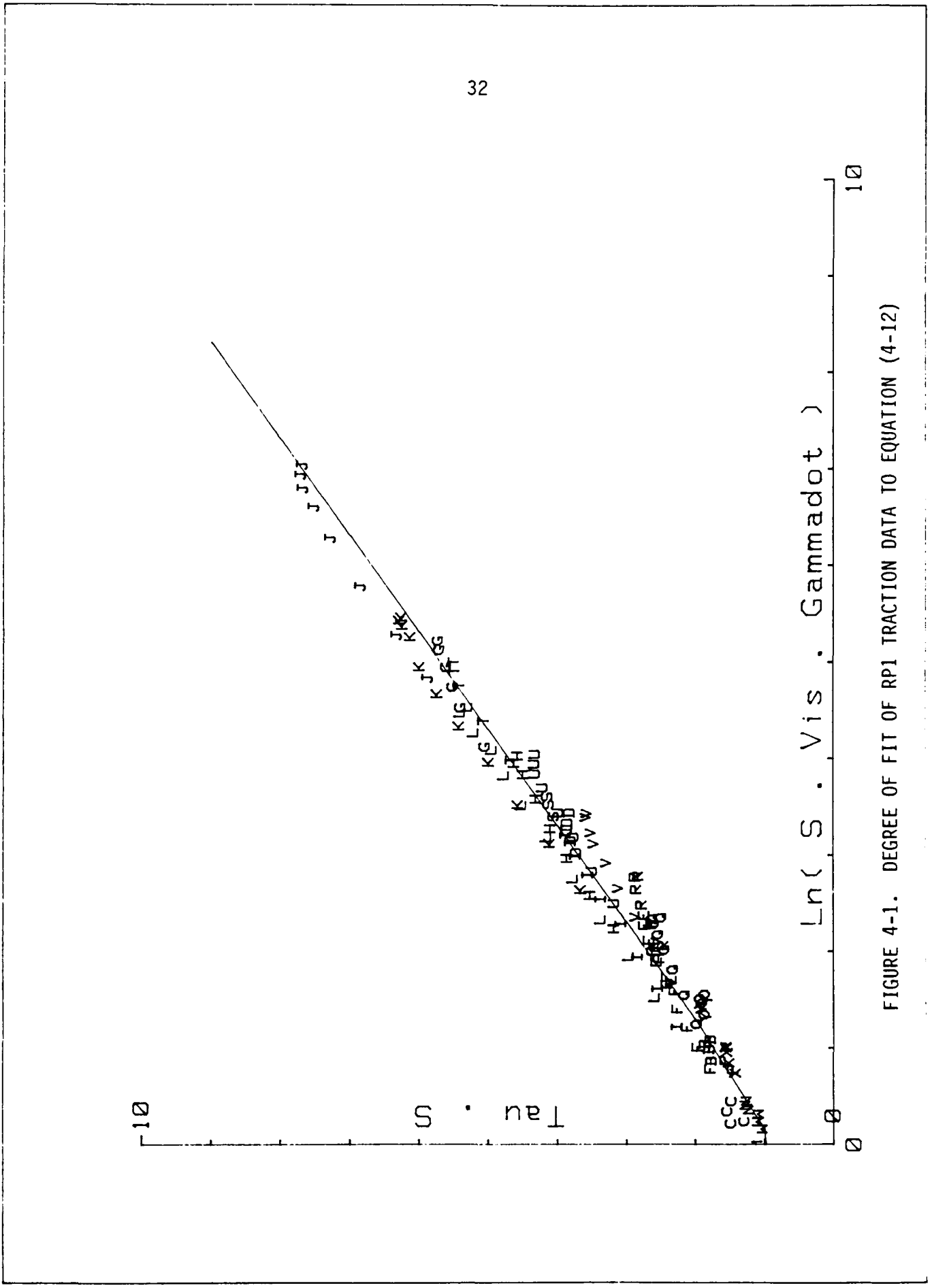

FIGURE 4-1. DEGREE OF FIT OF RP1 TRACTION DATA TO EQUATION (4-12)

5-0 TRACTION PREDICTION

The ultimate aim in obtaining the fluid rheological properties is to solve for the traction response of a concentrated contact under general conditions of slip, spin, and geometry. In this report we will restrict ourselves to the conditions of sideslip or longitudal slip only. Calculation methods for other contact kinematic conditions are outlined in Tevaarwerk [1979a] and Tevaarwerk [1979b].

As another way to observe the faithfulness of the traction modeling it may be instructive to predict the measured traction curves on the reduced data as extracted.

5-1 Comparison Between Measured and Predicted Traction

The process essentially involves the reverse operation to that used for the extraction of the traction parameters. Starting with Equation (3-8)

$$J4_t = J4_e + \frac{\tau_c}{\tau_o} J4_p \quad . \tag{3-8}$$

where, $J4_e = \dfrac{4\,S}{\pi(1+S^2)^2}$,

$$J4_p = \frac{2}{\pi}\left[\tan^{-1}S + \frac{S(S^2-1)}{(1+S^2)^2}\right], \text{ and}$$

$$S = \frac{2}{3}\,\frac{J1}{Ik} = \frac{2}{3}\,\frac{\bar{G}\,a\,\Delta U}{\tau_o\,h\,U}$$

As an average shear modulus $\bar{G}$ we have to use the combination of fluid shear modulus and the elastic compliance of the discs. This apparent modulus can be calculated from the compliance corrected modulus as given in Equation (4-17) together with the relationships (4-2), (4-3), and (4-4). This results in:

$$\bar{G} = \frac{G_c}{1 + \frac{8Qa\ G_c}{3\pi h G_s}} \qquad [Pa] \tag{5-1}$$

where,

G_c	=	compliance corrected modulus as given by Equation (4-17),	
a	=	semi contact size in rolling direction,	[m]
G_s	=	shear modulus of disc material,	[Pa]
Q	=	Kalker coefficient, and	[-]
h	=	central contact film thickness.	[m]

The average fluid shear strength τ_o based on the inlet temperature can be calculated directly from Equation (4-12) by using θ_o as the shear plane temperature,

$$\frac{\tau_o}{\theta_o + D_s} = \frac{1}{C}\left[\frac{A}{\theta_o + D_v} + \frac{BP}{\theta_o + D_p} + \mathrm{Ln}\left(\frac{2CV_o\ \Delta v}{(\theta_o + D_s)\ h}\right)\right], \text{ and} \tag{5-2}$$

using the fluid constants as given in Equation (4-19).

To solve for the ratio of fluid shear strength at the shear plane temperature θ_c and the inlet temperature θ_o requires a simple iteration since θ_c is a function of τ_c and vice-versa as indicated by Equations (3-9), (3-10), (3-11) and (4-12). Additional to the temperature dependence of τ_c through θ_c there is also the influence of thermal conductivity. In most cases only two or three iterations are needed for convergence. By using this technique, and the rheological data as extracted, the sideslip traction can be predicted for each of the measured traction curves. The comparison between measured and predicted traction may be observed from the graphs included in Appendix II. Overall the degree of predictions correlates very well with the experimentally observed results indicating a high degree of confidence in the traction modeling.

5-2 Traction Predictions for Line Contact

Traction prediction for line contact is essentially the same as that outlined in Section 5-1. The fundamental fluid parameters are independent of the exact contact geometry so there would be no change there. Changes do need to be made in the following:

1) Film thickness calculations,
2) Kalker correction factor,
3) Mean contact pressure, and
4) Shear plane temperature calculation.

The film thickness calculations should reflect the increased film that is found when rollers form a line contact. In the line contact calculations performed here, the central film thickness calculations according to Dowson-Higginson [1977] are used. The effect of the increased film thickness is a slight reduction in the traction in the thermal region because of increased thermal resistance of the thicker film as compared with elliptical contacts.

Kalker's correction factor for the compliance of the discs should now reflect the direction of the slip and the contact geometry. From Kalker [1967] we find that a value of Q for line contact is:

(5-3) $$Q = 0.6. \qquad [-]$$

When the traction data was fitted to the fluid rheological model, averaged quantities were used. The average pressure in a line contact is somewhat higher for a given peak contact pressure than in an elliptical contact. From Hertz stress considerations we can calculate a correction factor for line contact. Hence for the same peak Hertz pressure we should use a mean pressure that is about 18 percent higher in the traction calculations.

The shear plane calculations are based on Equation (3-9). This equation consists of two thermal resistance terms, 1) that due to the film, and 2) that due to the contact. The change in film resistance is taken care of by using the film thickness calculations for line contact. The change in contact resistance can be corrected for by using the ratio of contact resistance for circular contact and rectangular contact. Jaeger [1942] gives this ratio as:

$$\frac{R_{line}}{R_{circular}} \cong 1.05.$$

This is based on average contact temperature. Using the corrected terms in relevant equations, calculations identical to these for elliptical contact under side slip can be carried out.

5-2-1 Line Contact Traction Predictions

One of the aims of this investigation was to provide traction data on RP1 that can be used in the bearing analysis code SHABERTH. The traction data required by SHABERTH is in the form of a number of selected points from line contact traction test. The above outlined technique was used to modify the data obtained using elliptical contact traction tests into line contact data. Using this method the following line contact traction test curves were predicted.

Contact Pressure	P_o:	1.6, 2.3, 3.0,	[GPa]
Rolling Speed	U:	30, 60, 100,	[m/s]
Temperature	θ_o:	40, 75, 100, and	[°C]
Slide/Roll Ratio	$\frac{\Delta U}{U}$:	0.0 to 0.40,	[-]

The predicted line contact traction curves are included in Appendix III.

6-0 REFERENCES

Alsaad, M., Bair, S., Sandorn, D.M. and Winer, W.O., "Glass Transition in Lubricants: Its Relation to Elastohydrodynamic Lubrication", J. Lubr. Technol., Trans. ASME, [1978] pp. 404-417.

Bridgman, P.W., "The Physics of High Pressure", Dover Publications, Inc., New York, [1970].

Clark, O.H., Woods, W.W. and White, J.R., "Lubrication at Extreme Pressure with Mineral Oil Films", J. Appl. Phys. [1951], No. 4, pp. 474-483.

Conry, T.F., Johnson, K.L. and Owen, S., "Viscosity in the Thermal Regime of Traction", Proc. of the Leeds-Lyon Conference, Lyon [1979], pp. 219-227.

Daniels, B.K., "Non-Newtonian Thermo-Viscoelastic EHD Traction from Combined Slip and Spin", ASME Preprint 78-LC-2A-2. ASLE/ASME Lubrication Conference, Minneapolis, Minnesota, October 24-26, [1978].

Dowson, D., and Higginson, G.R., "Elasto-Hydrodynamic Lubrication", Pergammon Press, [1977].

Hamrock, B.J. and Dowson, D., "Isothermal Elastohydrodynamic Lubrication of Point Contacts, Part III - Fully Flooded Results", J. Lubr. Technol. Trans. ASME, [1977], No. 2, pp. 264-276.

Hirst, W. and Moore, A.J., "The Effect of Temperature on Traction in Elastohydrodynamic Lubrication", Phil. Trans. Roy. Soc. of London, Sept. 1980, Series A, No. 1438, pp. 183-208.

Jaeger, J.C., "Moving Sources of Heat and the Temperature at Sliding Contacts", Proc. R. Soc. New S.W., Vol. 56, p. 203, [1942].

Johnson, K.L., "Introductory Review of Lubricant Rheology and Traction", Proc. of the Leeds-Lyon Conference, Leeds [1978], pp. 155-161.

Johnson, K.L. and Cameron, R., "Shear Behavior of Elastohydrodynamic Oil Films at High Rolling Contact Pressures", Proc. Inst. Mech. Eng. (London), No. 14, [1967], pp. 307-319.

Johnson, K.L., and Greenwood, J.A., "Thermal Analysis of an Eyring Fluid in EHL Traction", Wear, [1980], p 353.

Johnson, K.L. and Roberts, A.D., "Observations of Viscoelastic Behavior of an Elastohydrodynamic Lubricant Film", Proc. Roy. Soc. (London), Series A, No. 1609, [1974], pp. 217-242.

Johnson, K.L. and Tevaarwerk, J.L., "Shear Behavior of Elastohydrodynamic Oil Films", Proc. Roy. Soc. (London), Series A, No. 1609, [1977], pp. 215-236.

Kalker, J.J., "On the Rolling Contact of Two Elastic Bodies in the Presence of Dry Friction", Ph.D. Dissertation, Technische Hogeschool, Delft, [1967].

Liquid Propellant Manual CPIA/M4, Chemical Propulsion Agency, Johns Hopkins University, Laurel, MD, [1982].

Murch, L.E., and Wilson, W.R.D., "A Thermal Elastohydrodynamic inlet zone analysis.", J. Lubr. Technol. Trans. ASME, [1975], No. 2, p. 212.

Niemann, G. and Stoessel, K., "Reibungszahlen Bei Elasto-Hydrodynamisher Schmierung in Reibrad-und Zahnradgetrieben", Konstruktion, No. 7, [1971], pp. 245-260.

Smith, F.W., "Rolling Contact Lubrication-The Application of Elasto-Hydrodynamic Theory", Trans. Am. Soc. Mech. Engrs., [1965], Series D, p. 170.

Smith, R.L., Walowit, J.A. and McGrew, J.M., "Elastohydrodynamic Traction Characteristics of 5P4E Polyphenyl Ether", J. Lubr. Technol. Trans. ASME, [1973], pp. 353-362.

Tevaarwerk, J.L., "Traction Drive Performance Prediction for the Johnson and Tevaarwerk Traction Model", NASA TP-1530, [1979a].

Tevaarwerk, J.L. and Johnson, K.L., "The Influence of Fluid Rheology on the Performance of Traction Drives", J. Lubr. Technol. Trans. ASME, [1979b], p 266.

Tevaarwerk, J.L., "Traction Calculations using the Shear Plane Hypothesis", Proc. of the Leeds-Lyon Conference, Lyon [1979c], pp. 201-213.

Tevaarwerk, J.L., "Thermal Influence on the Traction Behavior of an Elastic/Plastic Model", Proc. of the Leeds-Lyon Conference, Leeds [1980], pp. 302-309.

Tevaarwerk, J.L., "A Simple Thermal Correction for Large Spin Traction Curves" J. Mech. Design. Trans. ASME, [1981], p. 440.

Tevaarwerk, J.L., "Thermal Traction Contact Performance Evaluation Under Fully Flooded and Starved Conditions", NASA CR-168173, May, [1983].

Tevaarwerk, J.L., "Constitutive Modelling of Lubricants in Concentrated Contacts at High Slide to Roll Ratio", NASA-CR-175029, [1985].

Vargaftik, N.B., "Handbook of Physical Properties of Liquids and Gases", 2nd Edition, Washington, Hemisphere Publishing Corp., [1983].

APPENDIX I

ORIGINAL MEASURED TRACTION DATA

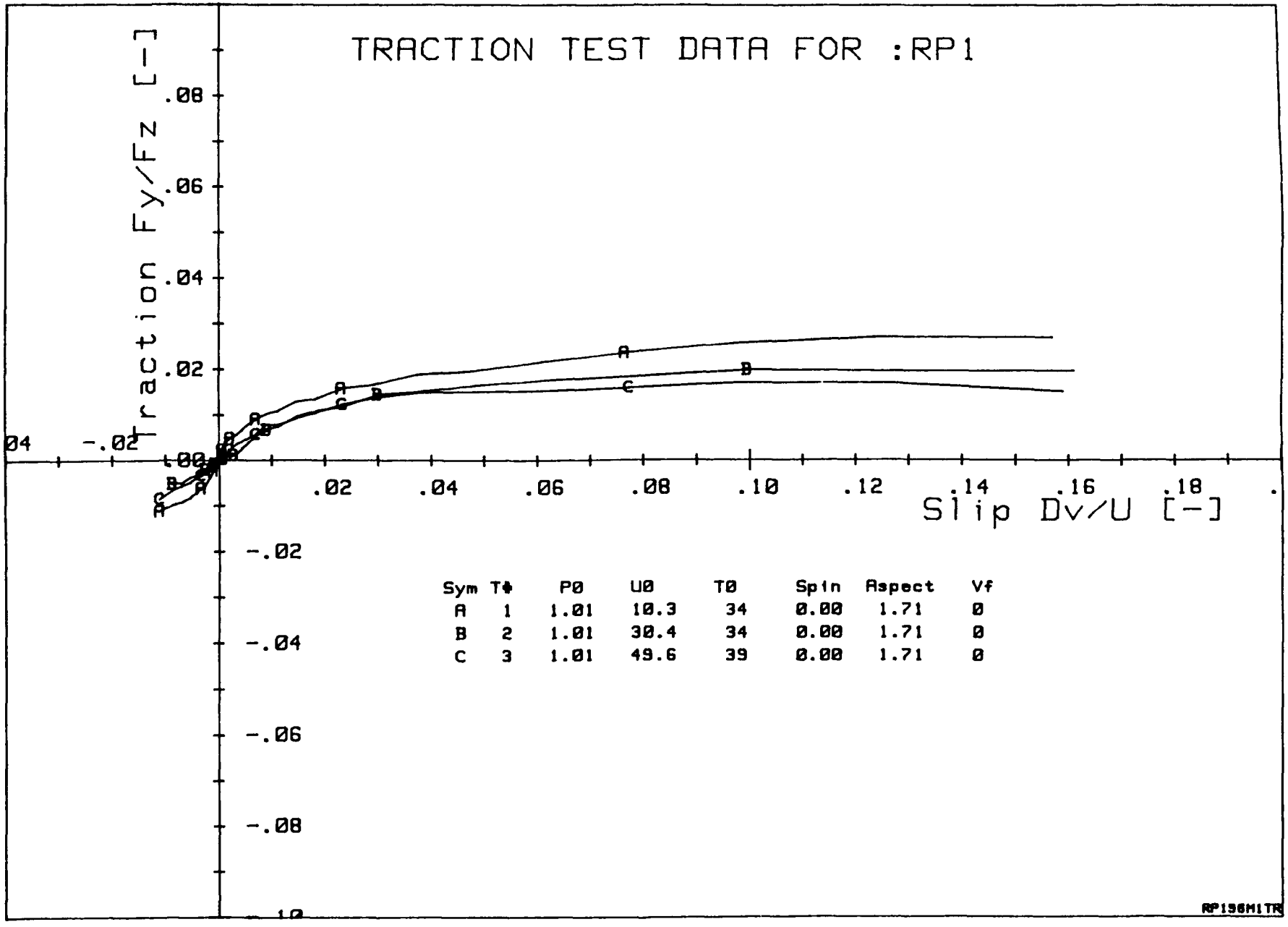
TRACTION TEST DATA FOR :RP1
Traction Fy/Fz [-]
.08
.06
.04
.02
-.02
-.04
-.06
-.08
.02
.04
.06
.08
.10
.12
.14
.16
.18
Slip Dv/U [-]
Sym T# P0 U0 T0 Spin Aspect Vf
A 1 1.01 10.3 34 0.00 1.71 0
B 2 1.01 30.4 34 0.00 1.71 0
C 3 1.01 49.6 39 0.00 1.71 0
RP19GMITR

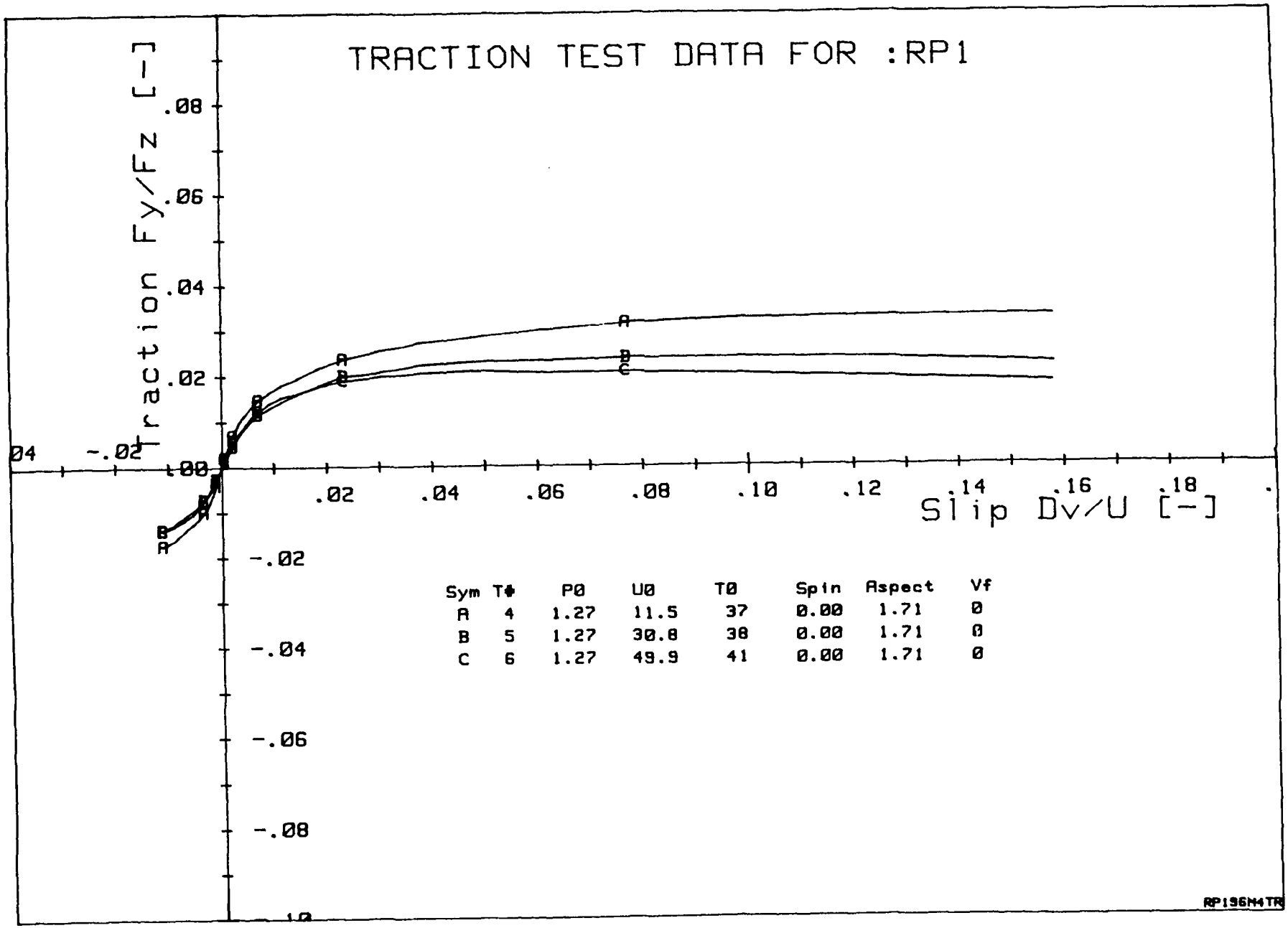
TRACTION TEST DATA FOR :RP1
Traction Fy/Fz [-]
.08
.06
.04
.02
-.02
-.04
-.06
-.08
.02
.04
.06
.08
.10
.12
.14
.16
.18
Slip Dv/U [-]
Sym T# P0 U0 T0 Spin Aspect Vf
A 4 1.27 11.5 37 0.00 1.71 0
B 5 1.27 30.8 38 0.00 1.71 0
C 6 1.27 49.9 41 0.00 1.71 0
RP196M4TR

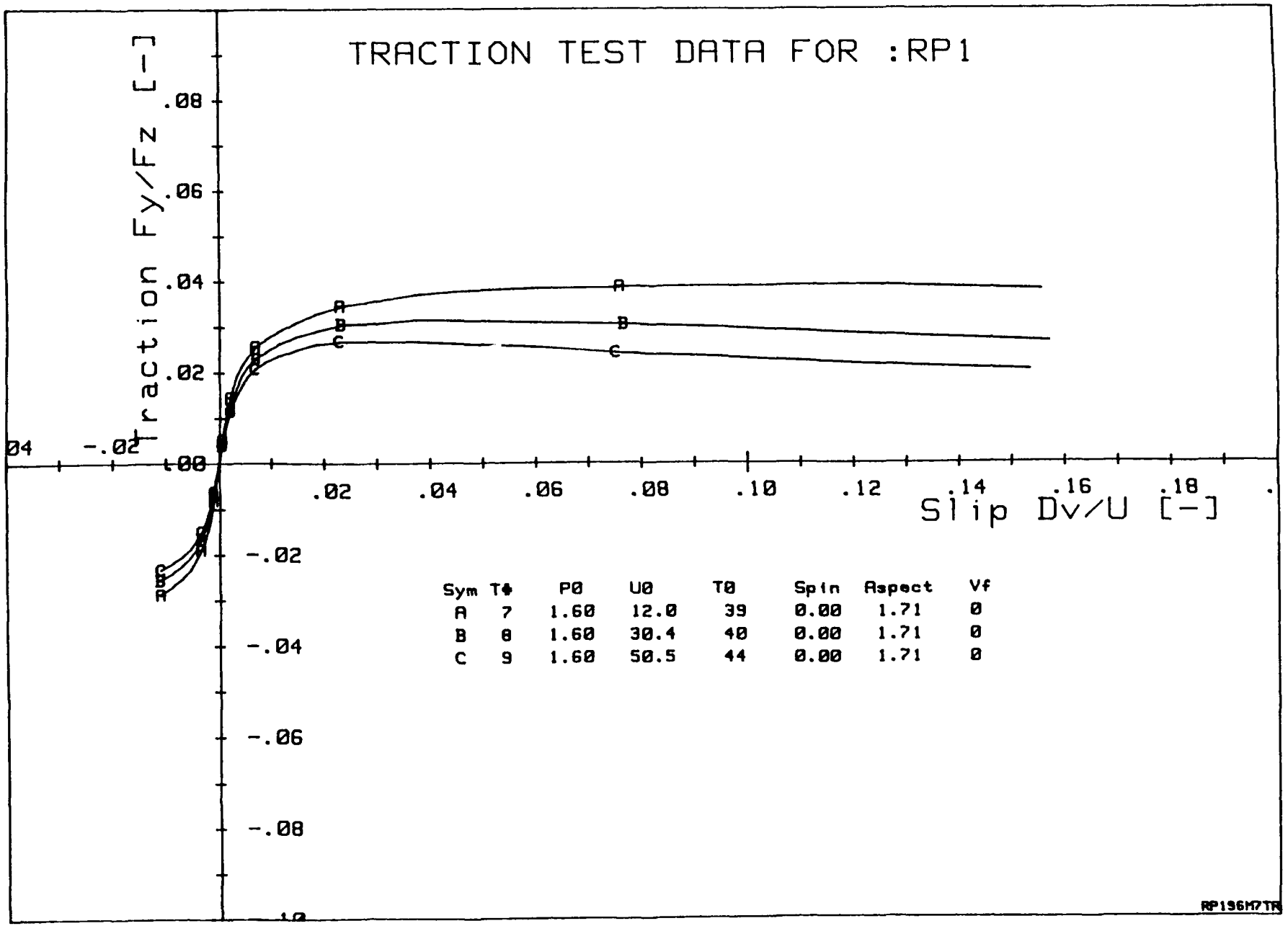
TRACTION TEST DATA FOR :RP1
Traction Fy/Fz [-]
.08
.06
.04
.02
-.02
-.04
-.06
-.08
.02
.04
.06
.08
.10
.12
.14
.16
.18
Slip Dv/U [-]
A
B
C
Sym T# P0 U0 T0 Spin Aspect Vf
A 7 1.60 12.0 39 0.00 1.71 0
B 8 1.60 30.4 40 0.00 1.71 0
C 9 1.60 50.5 44 0.00 1.71 0
RP196M7TR

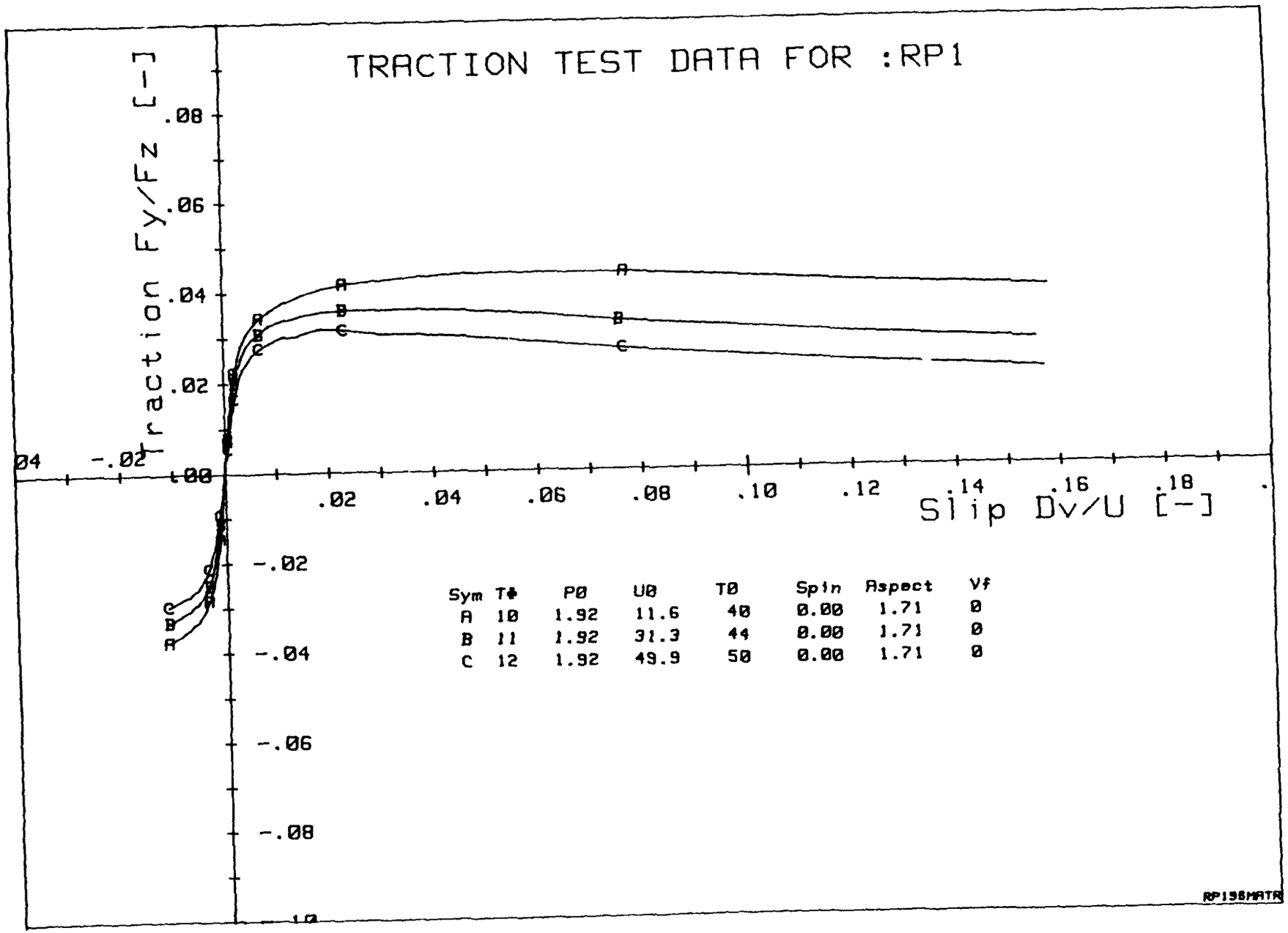
TRACTION TEST DATA FOR :RP1
Traction Fy/Fz [-]
.08
.06
.04
.02
-.02
-.04
-.06
-.08
.02
.04
.06
.08
.10
.12
.14
.16
.18
Slip Dv/U [-]
Sym T# P0 U0 T0 Spin Aspect Vf
A 10 1.92 11.6 40 0.00 1.71 0
B 11 1.92 31.3 44 0.00 1.71 0
C 12 1.92 49.9 50 0.00 1.71 0
RP195MATR

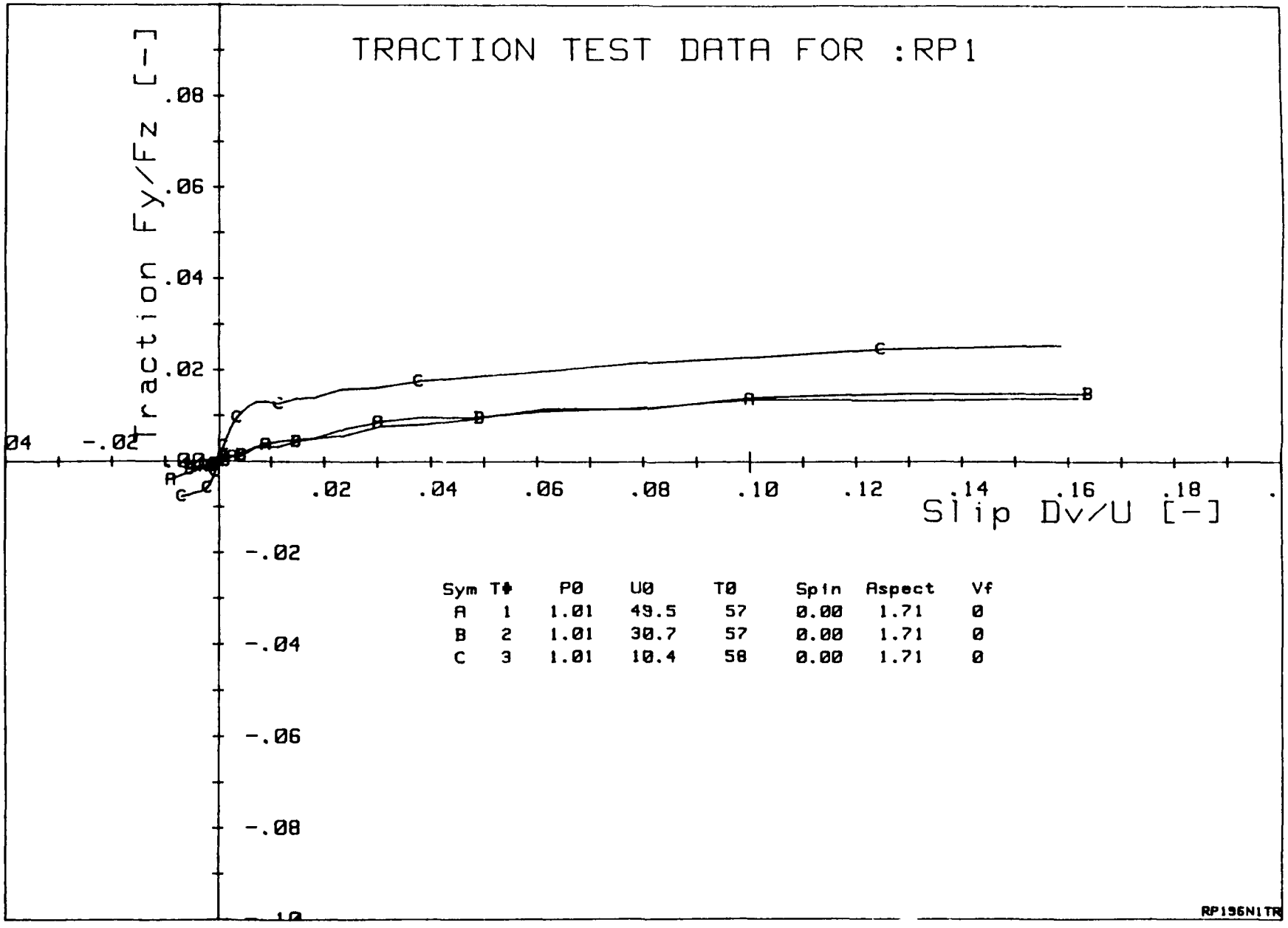
TRACTION TEST DATA FOR :RP1
Traction Fy/Fz [-]
.08
.06
.04
.02
-.02
-.04
-.06
-.08
.02
.04
.06
.08
.10
.12
.14
.16
.18
Slip Dv/U [-]
Sym T# P0 U0 T0 Spin Aspect Vf
A 1 1.01 49.5 57 0.00 1.71 0
B 2 1.01 30.7 57 0.00 1.71 0
C 3 1.01 10.4 58 0.00 1.71 0
RP196N1TR

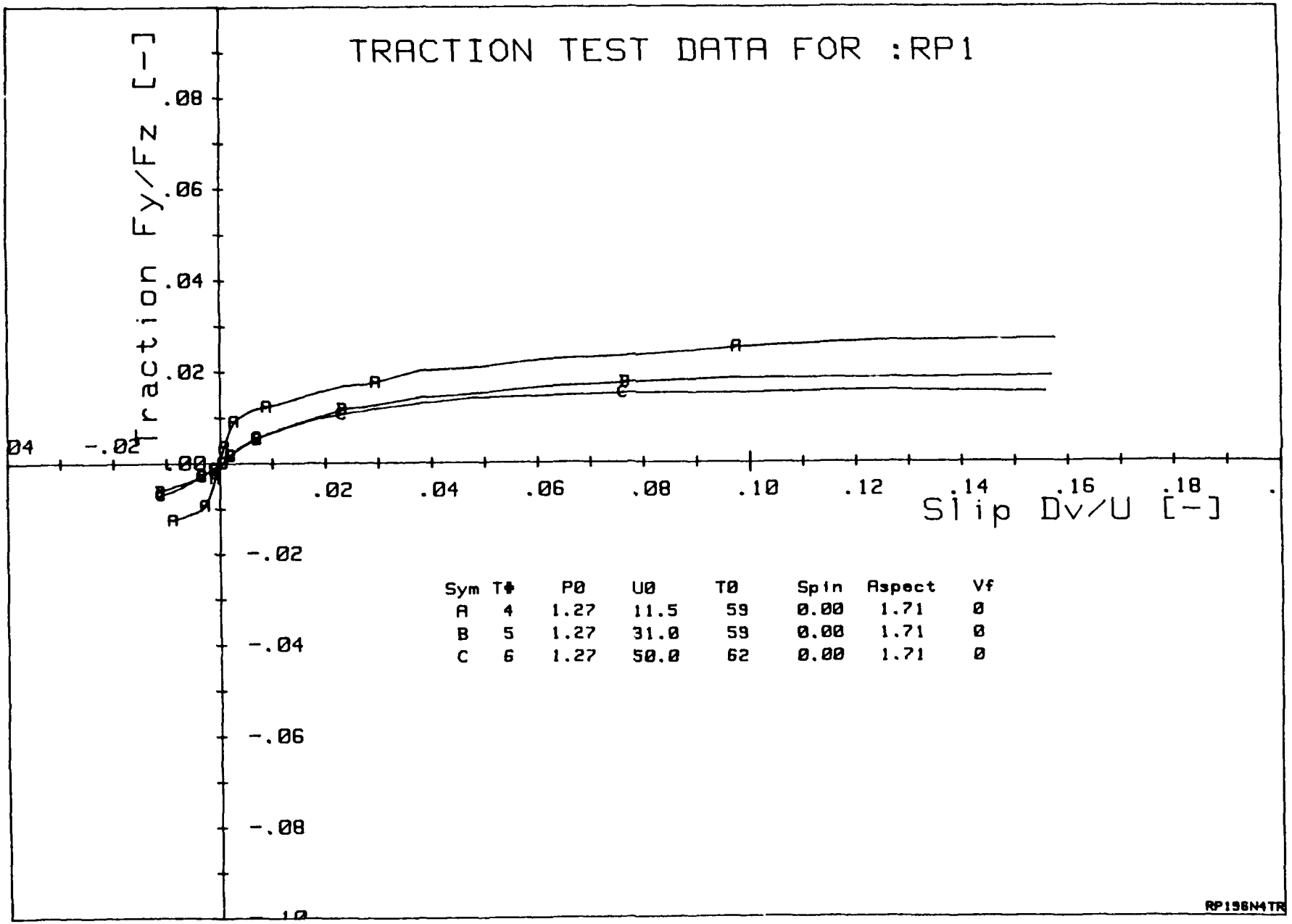
TRACTION TEST DATA FOR :RP1
Traction Fy/Fz [-]
.08
.06
.04
.02
-.02
-.04
-.06
-.08
.02
.04
.06
.08
.10
.12
.14
.16
.18
Slip Dv/U [-]
Sym T# P0 U0 T0 Spin Aspect Vf
A 4 1.27 11.5 59 0.00 1.71 0
B 5 1.27 31.0 59 0.00 1.71 0
C 6 1.27 50.0 62 0.00 1.71 0
RP19BN4TR

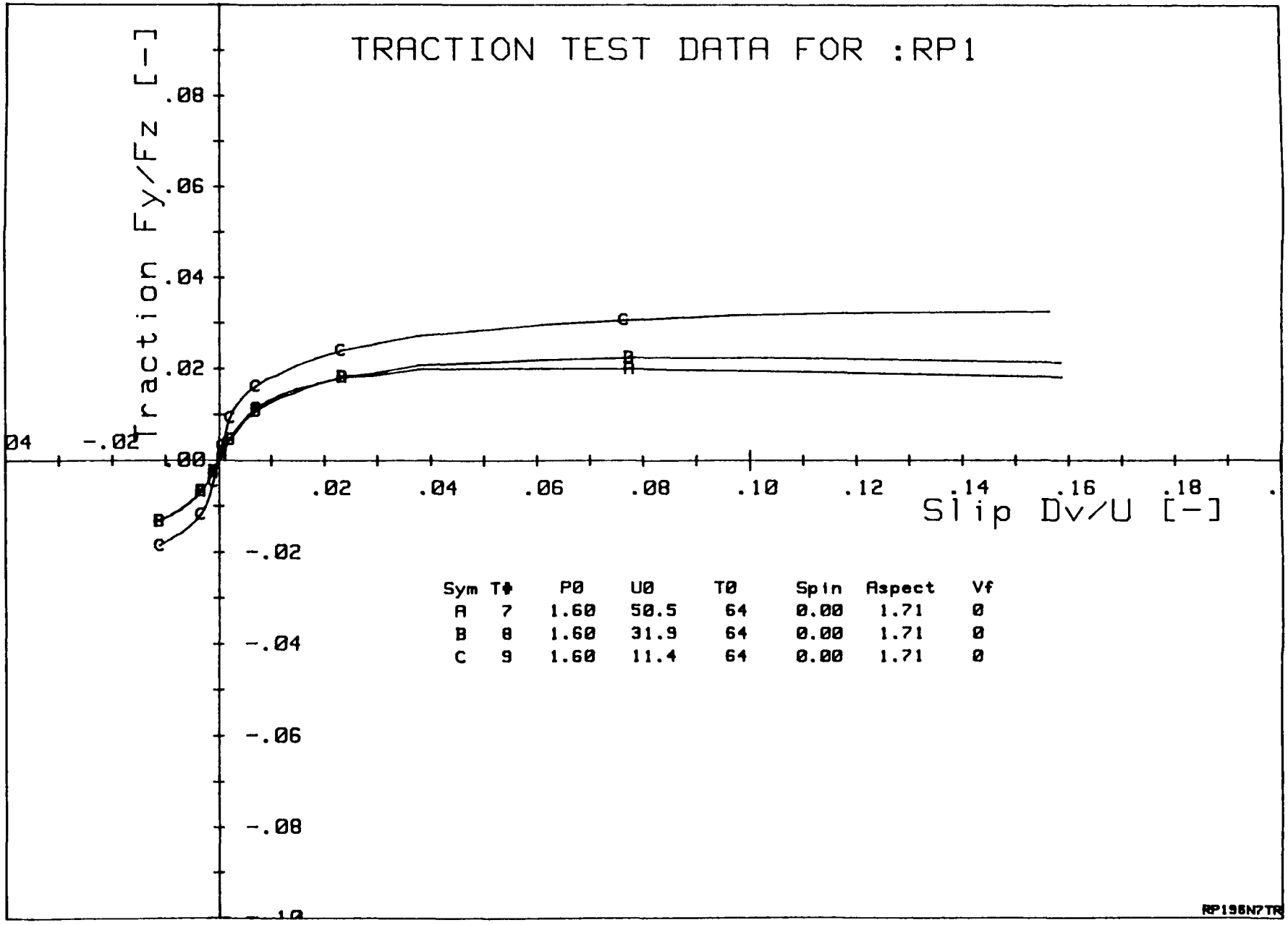
TRACTION TEST DATA FOR :RP1
Traction Fy/Fz [-]
.08
.06
.04
.02
-.02
-.04
-.06
-.08
.02
.04
.06
.08
.10
.12
.14
.16
.18
Slip Dv/U [-]
Sym T# P0 U0 T0 Spin Aspect Vf
A 7 1.60 50.5 64 0.00 1.71 0
B 8 1.60 31.9 64 0.00 1.71 0
C 9 1.60 11.4 64 0.00 1.71 0
RP195N7TR

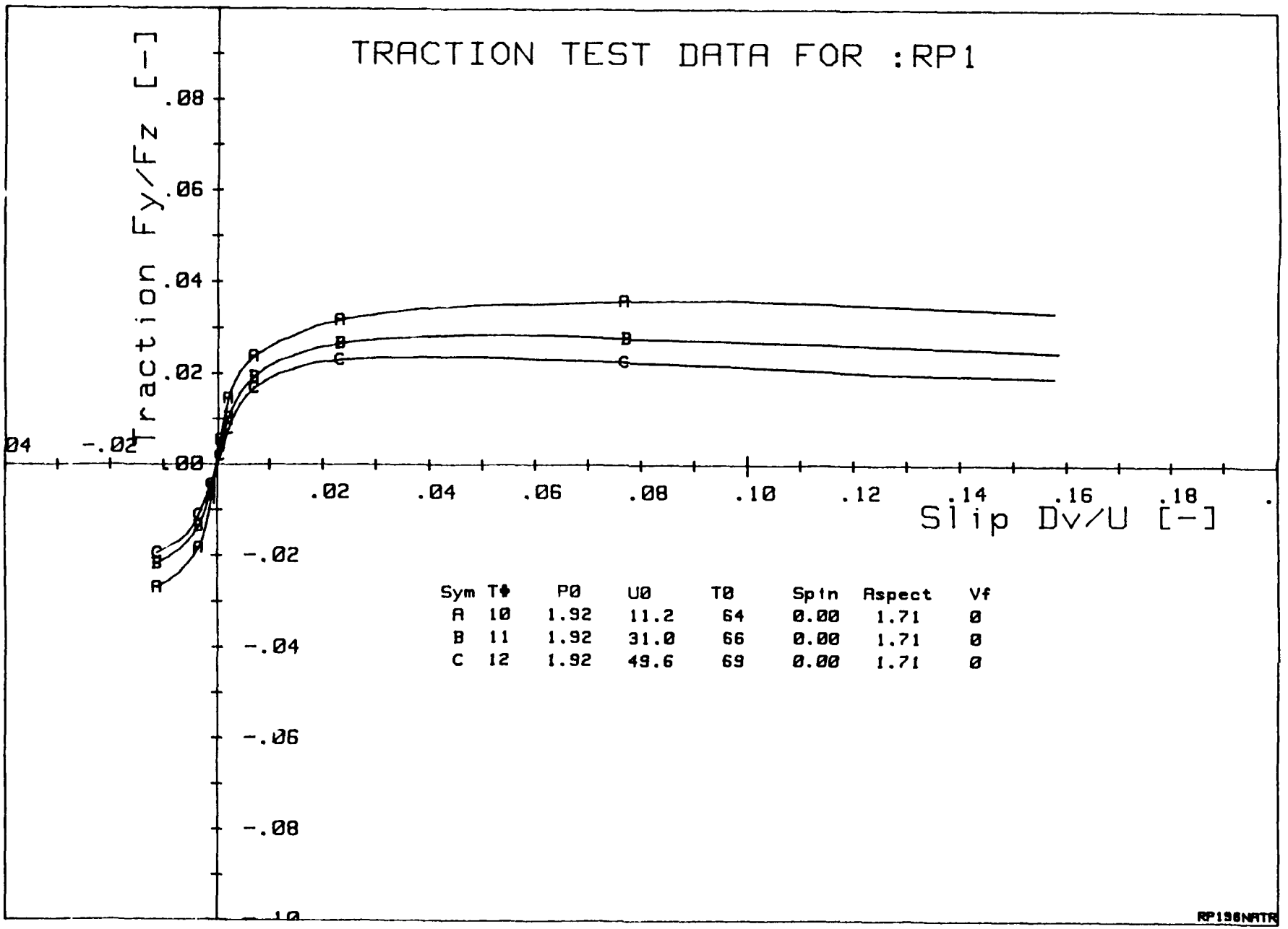
TRACTION TEST DATA FOR :RP1
Traction Fy/Fz [-]
.08
.06
.04
.02
-.02
-.04
-.06
-.08
-.10
.02
.04
.06
.08
.10
.12
.14
.16
.18
Slip Dv/U [-]
A
B
C
Sym T# P0 U0 T0 Spin Aspect Vf
A 10 1.92 11.2 64 0.00 1.71 0
B 11 1.92 31.0 66 0.00 1.71 0
C 12 1.92 49.6 69 0.00 1.71 0
RP19ANATR

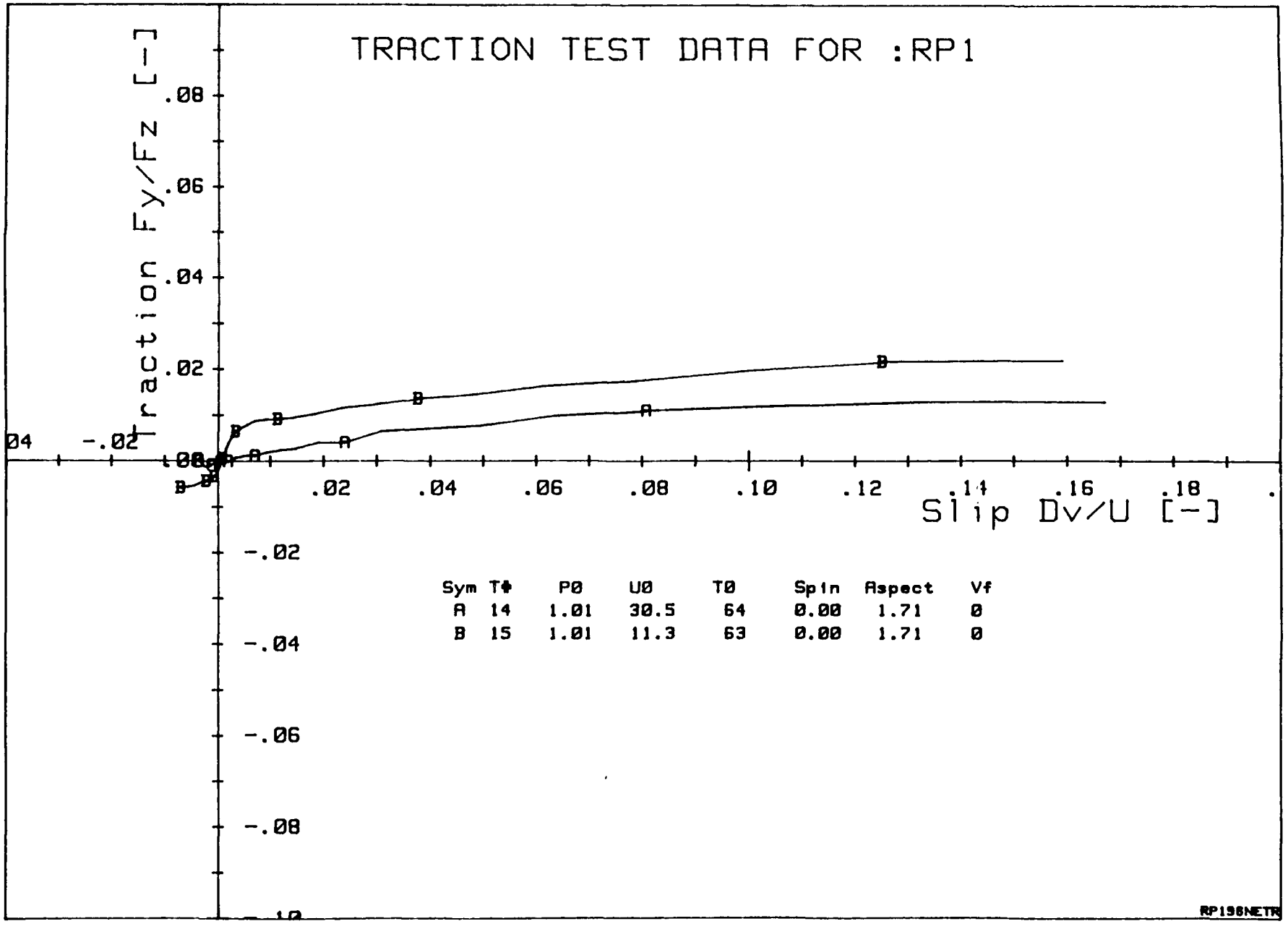
TRACTION TEST DATA FOR :RP1
Traction Fy/Fz [-]
.08
.06
.04
.02
-.02
-.04
-.06
-.08
.02
.04
.06
.08
.10
.12
.14
.16
.18
Slip Dv/U [-]
Sym T# P0 U0 T0 Spin Aspect Vf
A 14 1.01 30.5 64 0.00 1.71 0
B 15 1.01 11.3 63 0.00 1.71 0
RP19BNETR

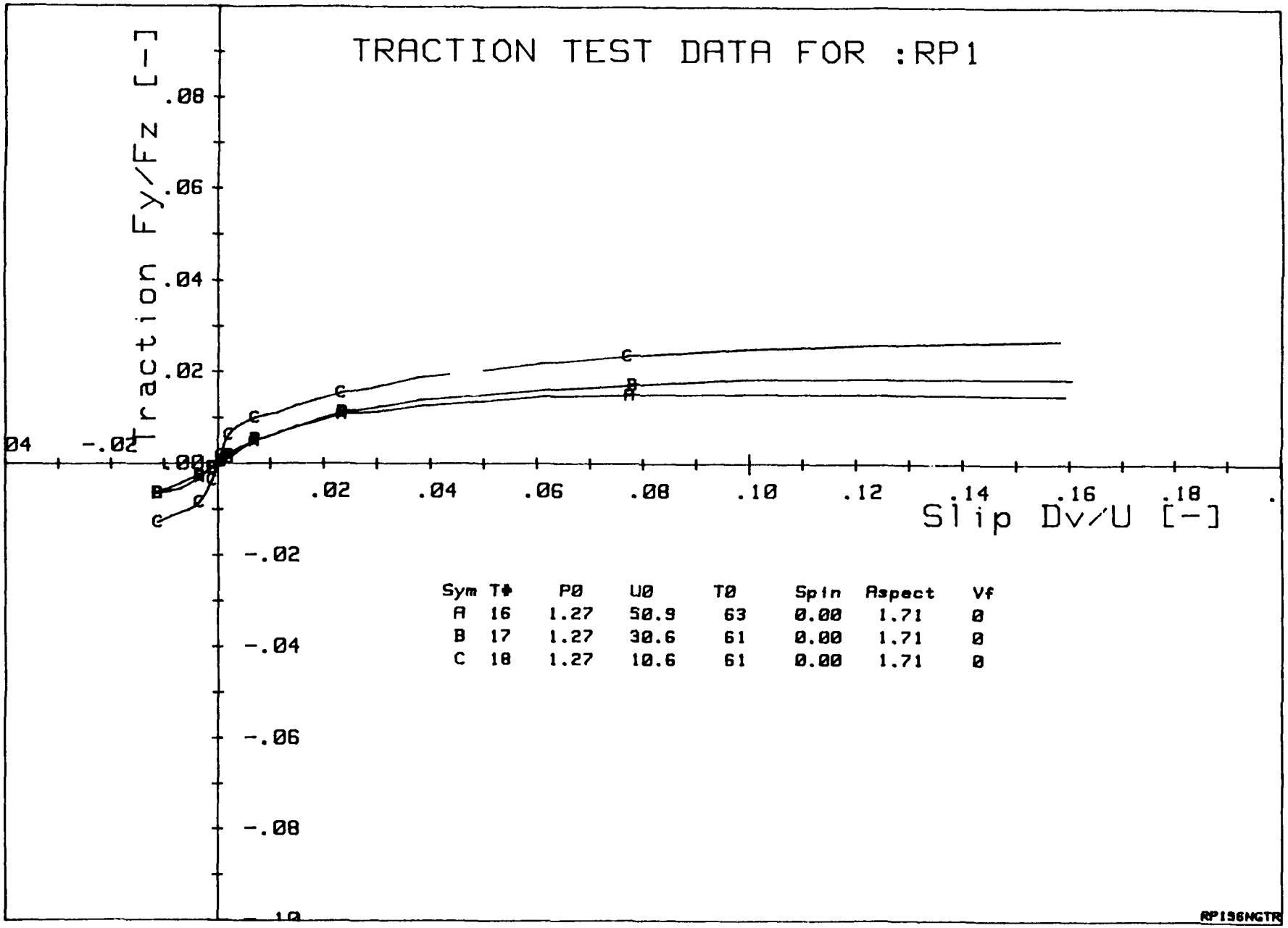
TRACTION TEST DATA FOR :RP1
Traction Fy/Fz [-]
.08
.06
.04
.02
.00
-.02
-.04
-.06
-.08
-.10
.02
.04
.06
.08
.10
.12
.14
.16
.18
Slip Dv/U [-]
Sym T# P0 U0 T0 Spin Aspect Vf
A 16 1.27 50.9 63 0.00 1.71 0
B 17 1.27 30.6 61 0.00 1.71 0
C 18 1.27 10.6 61 0.00 1.71 0
RP196NGTR

APPENDIX II

COMPARISON BETWEEN MEASURED AND PREDICTED ELLIPTICAL CONTACT DATA

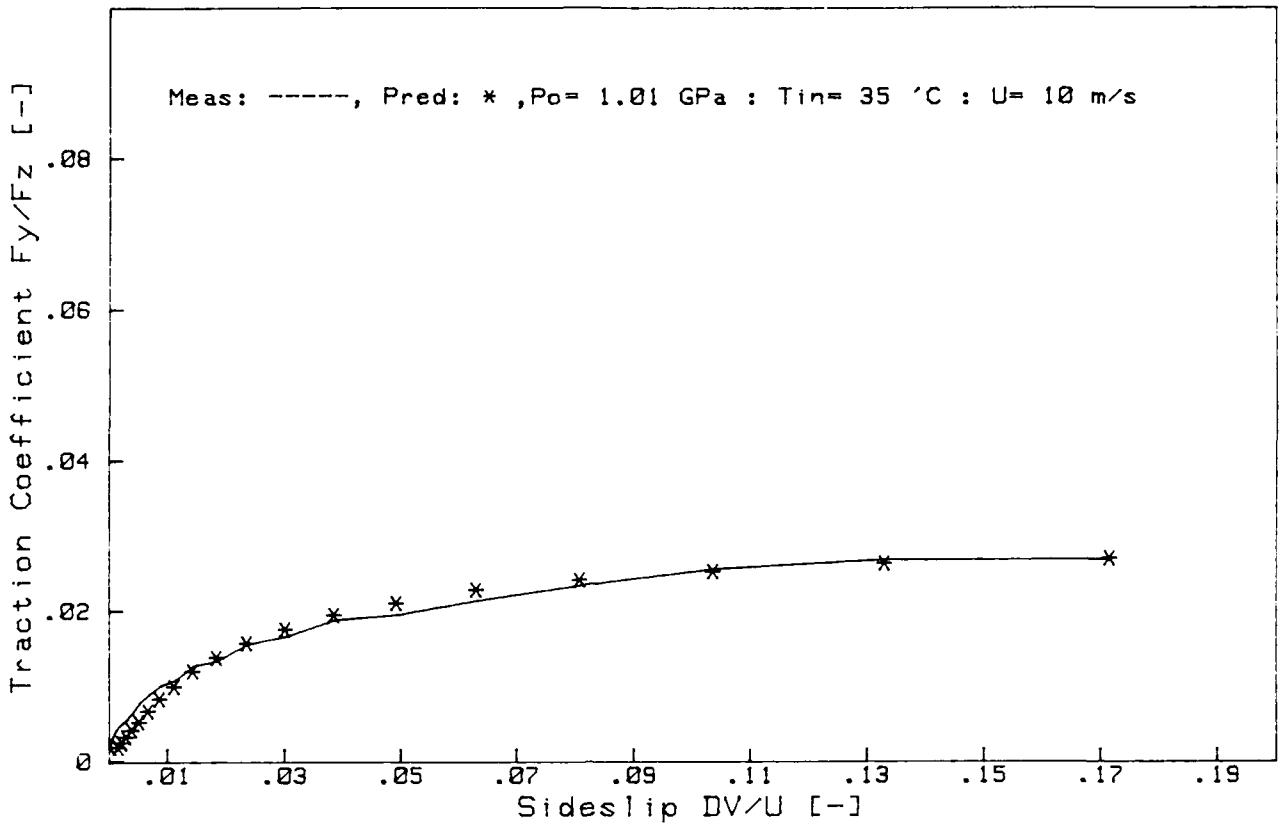
Meas: -----, Pred: * ,Po= 1.01 GPa : Tin= 35 'C : U= 10 m/s
Traction Coefficient Fy/Fz [-]
.08
.06
.04
.02
0
.01
.03
.05
.07
.09
.11
.13
.15
.17
.19
Sideslip DV/U [-]

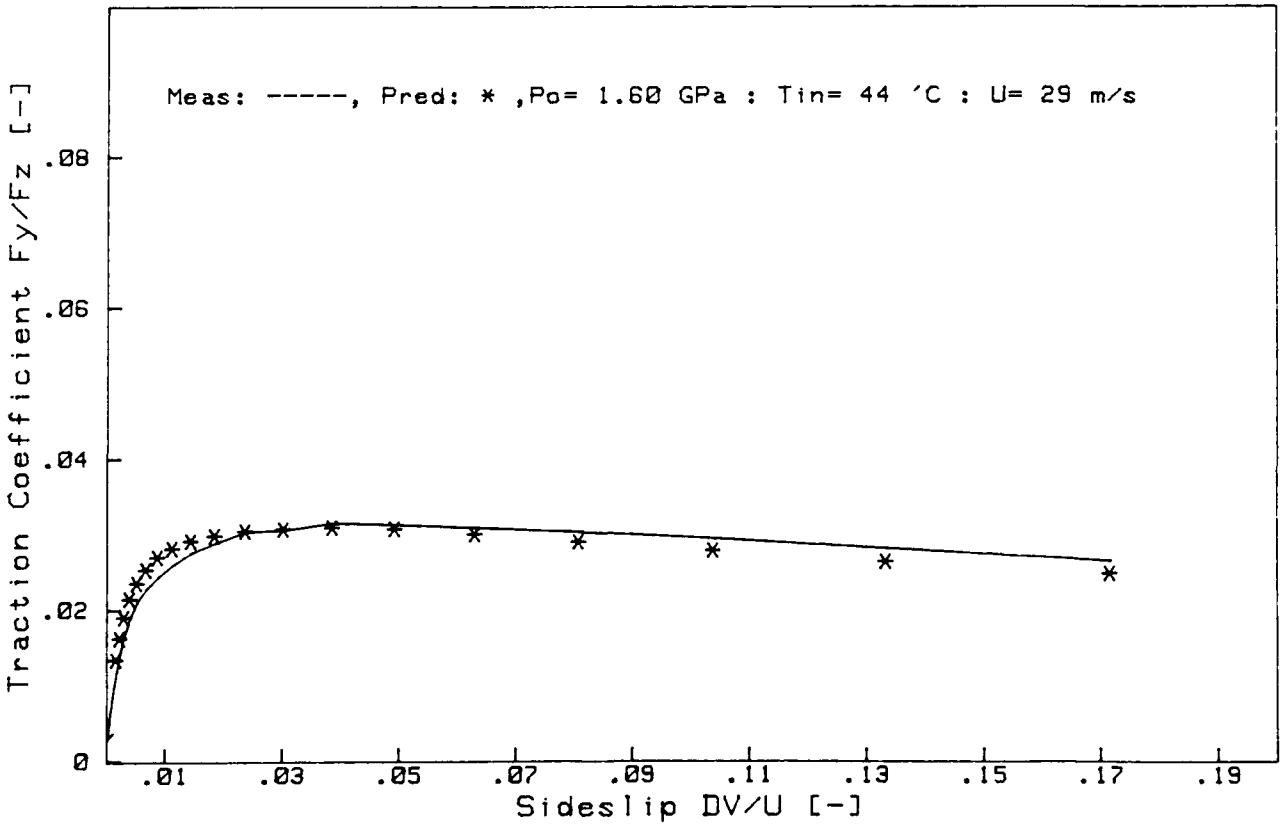
Meas: -----, Pred: * ,Po= 1.60 GPa : Tin= 44 'C : U= 29 m/s
Traction Coefficient Fy/Fz [-]
.08
.06
.04
.02
0
.01
.03
.05
.07
.09
.11
.13
.15
.17
.19
Sideslip DV/U [-]

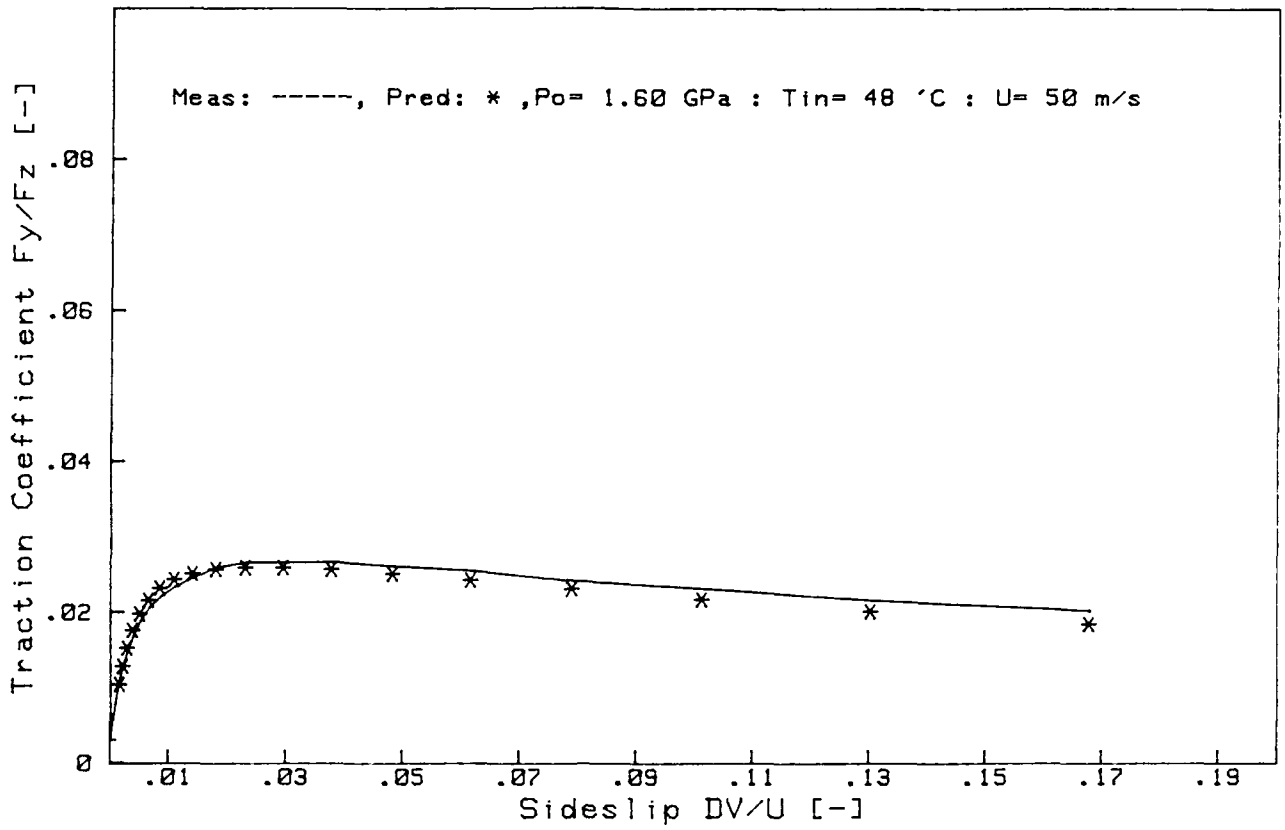
Meas: -----, Pred: * ,Po= 1.60 GPa : Tin= 48 'C : U= 50 m/s
Traction Coefficient Fy/Fz [-]
.08
.06
.04
.02
0
.01
.03
.05
.07
.09
.11
.13
.15
.17
.19
Sideslip DV/U [-]

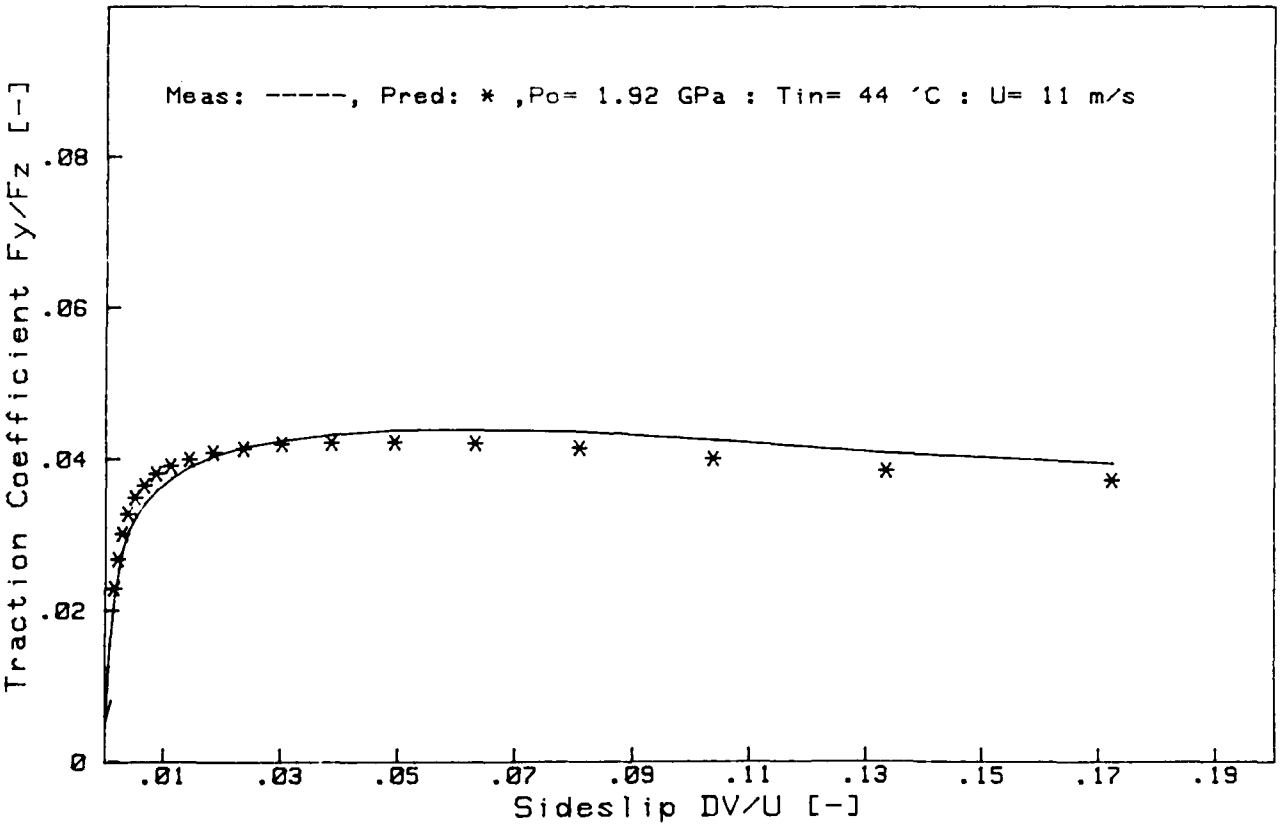
Meas: -----, Pred: * ,Po= 1.92 GPa : Tin= 44 'C : U= 11 m/s
Traction Coefficient Fy/Fz [-]
.08
.06
.04
.02
0
.01
.03
.05
.07
.09
.11
.13
.15
.17
.19
Sideslip DV/U [-]

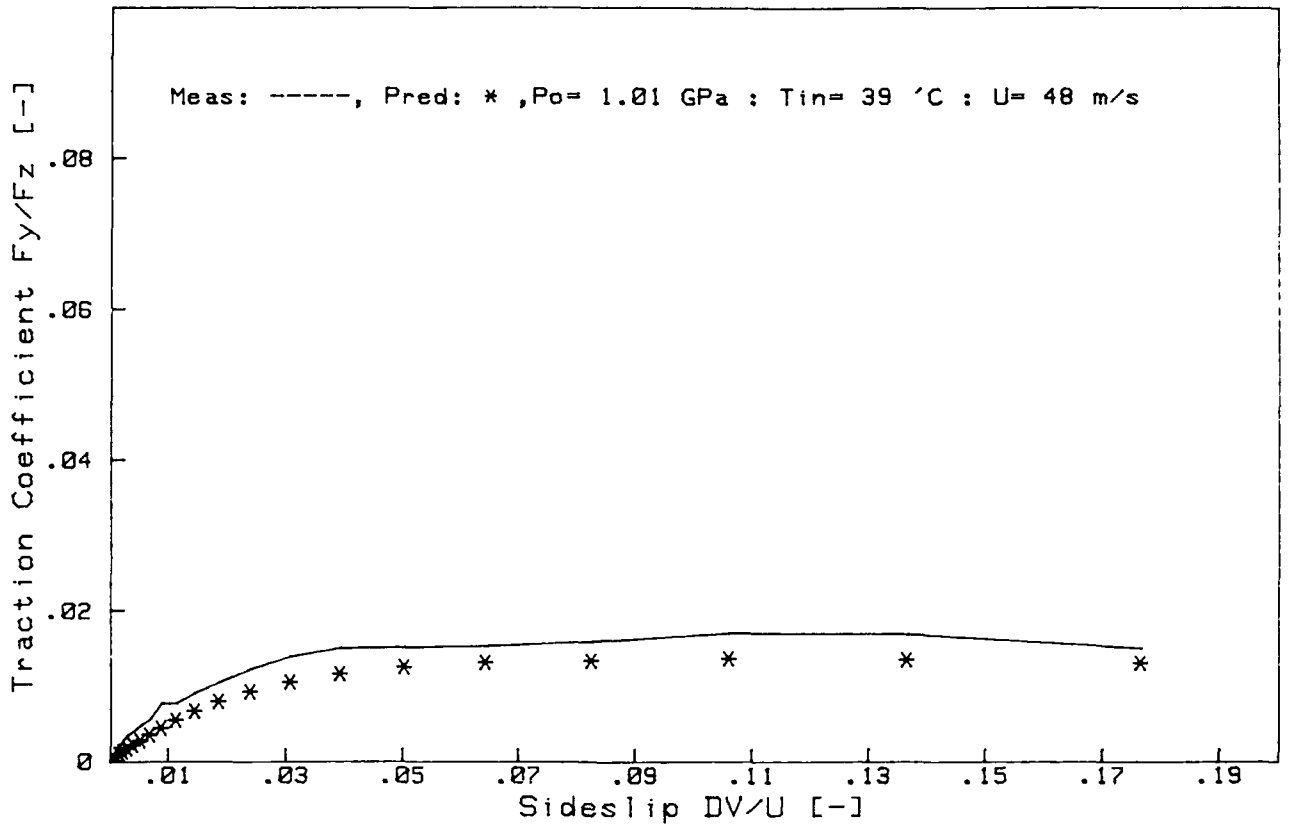
Meas: -----, Pred: * ,Po= 1.01 GPa : Tin= 39 'C : U= 48 m/s
Traction Coefficient Fy/Fz [-]
.08
.06
.04
.02
0
.01
.03
.05
.07
.09
.11
.13
.15
.17
.19
Sideslip DV/U [-]

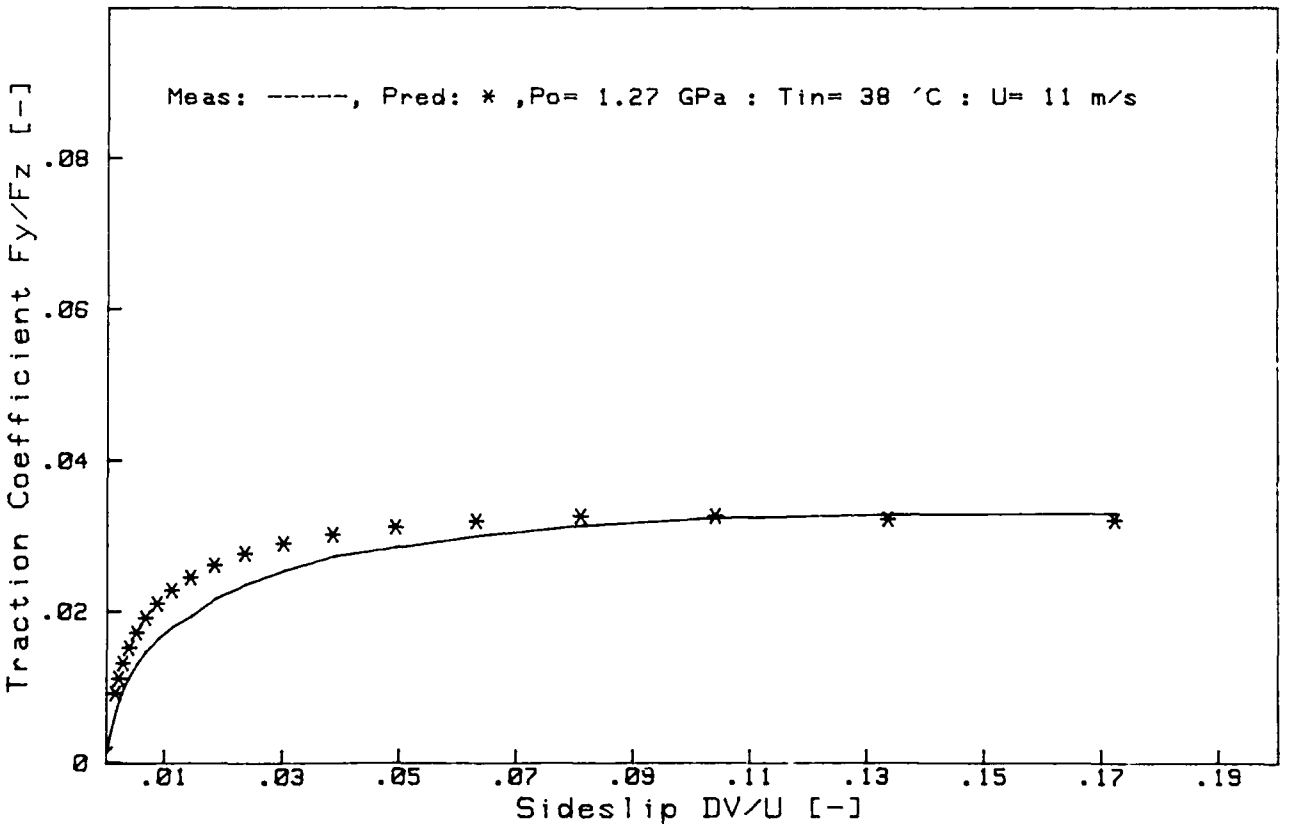
Meas: -----, Pred: * ,Po= 1.27 GPa : Tin= 38 'C : U= 11 m/s
Traction Coefficient Fy/Fz [-]
.08
.06
.04
.02
0
.01
.03
.05
.07
.09
.11
.13
.15
.17
.19
Sideslip DV/U [-]

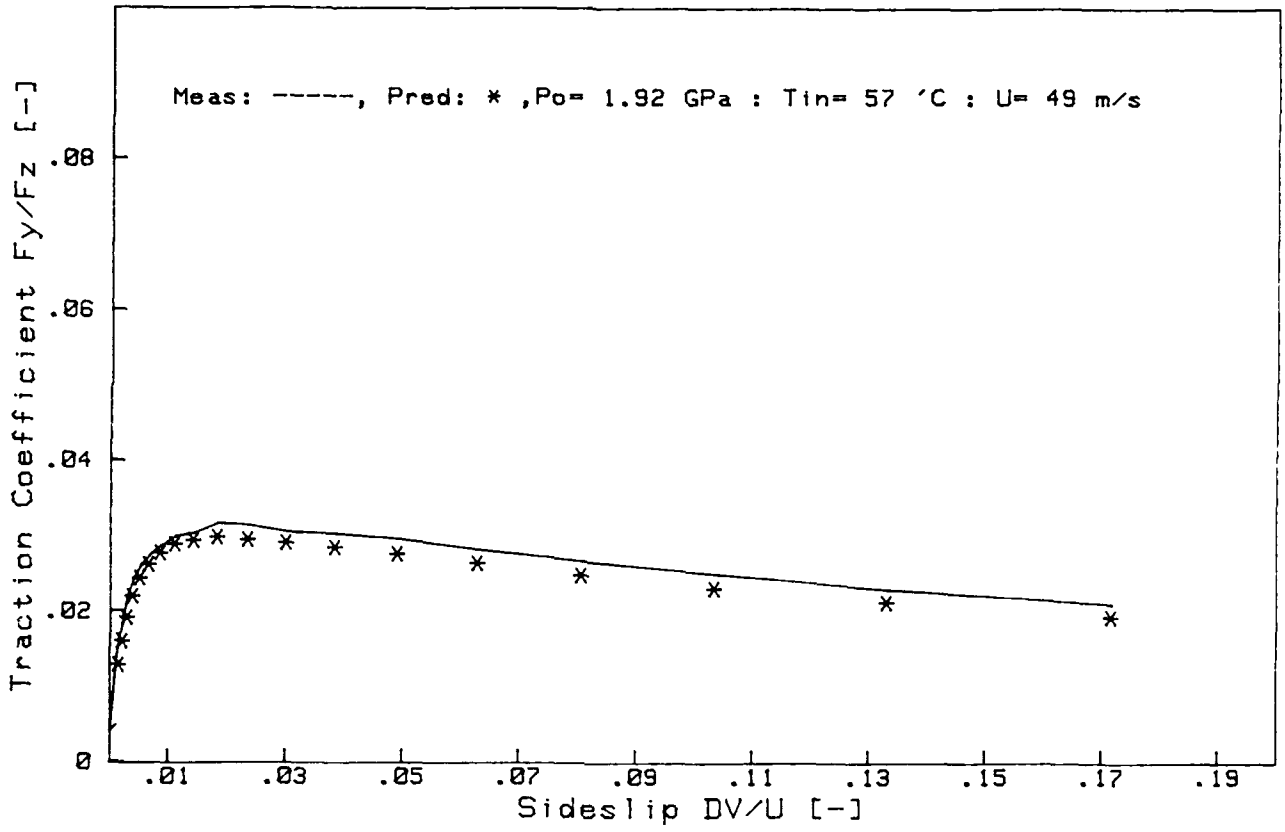
Meas: -----, Pred: * ,Po= 1.92 GPa : Tin= 57 'C : U= 49 m/s
Traction Coefficient Fy/Fz [-]
.08
.06
.04
.02
0
.01
.03
.05
.07
.09
.11
.13
.15
.17
.19
Sideslip DV/U [-]

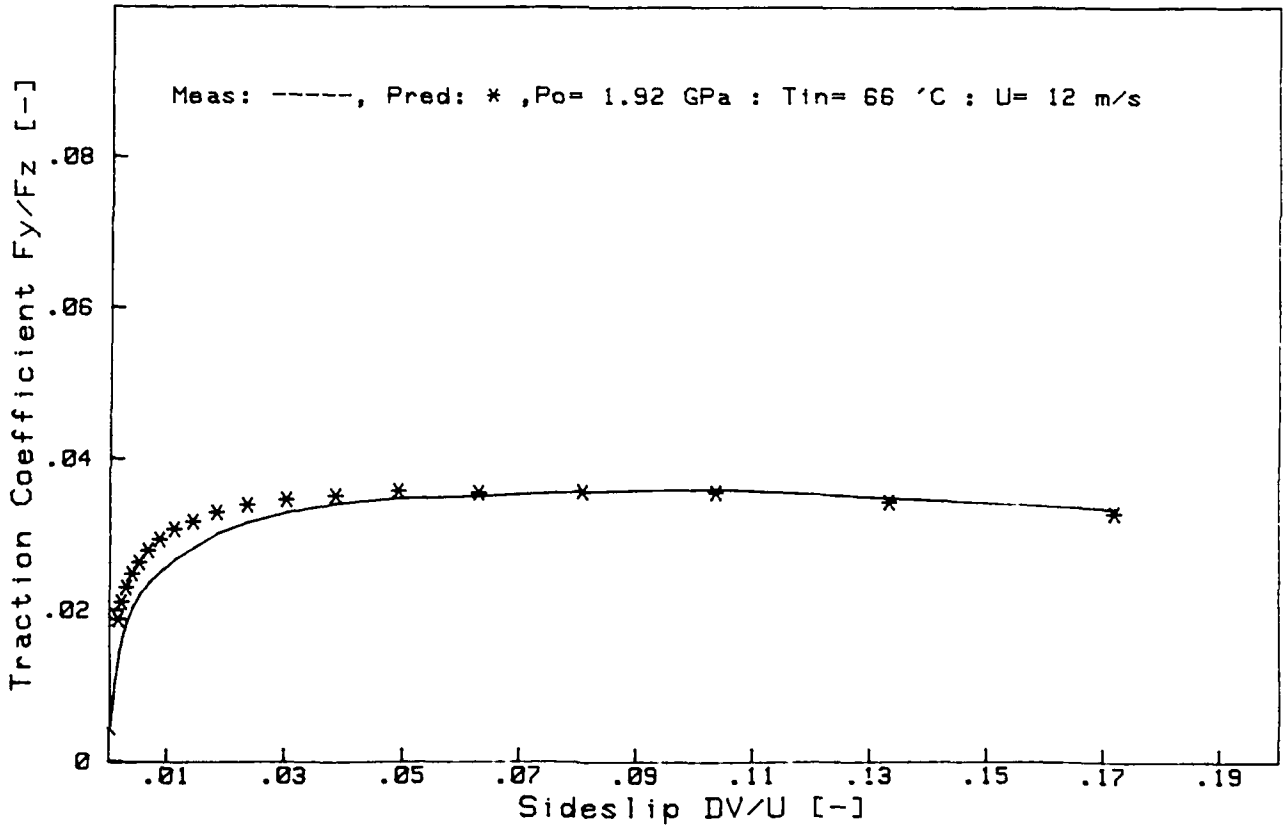
Meas: -----, Pred: * ,Po= 1.92 GPa : Tin= 66 'C : U= 12 m/s
Traction Coefficient Fy/Fz [-]
.08
.06
.04
.02
0
.01
.03
.05
.07
.09
.11
.13
.15
.17
.19
Sideslip DV/U [-]

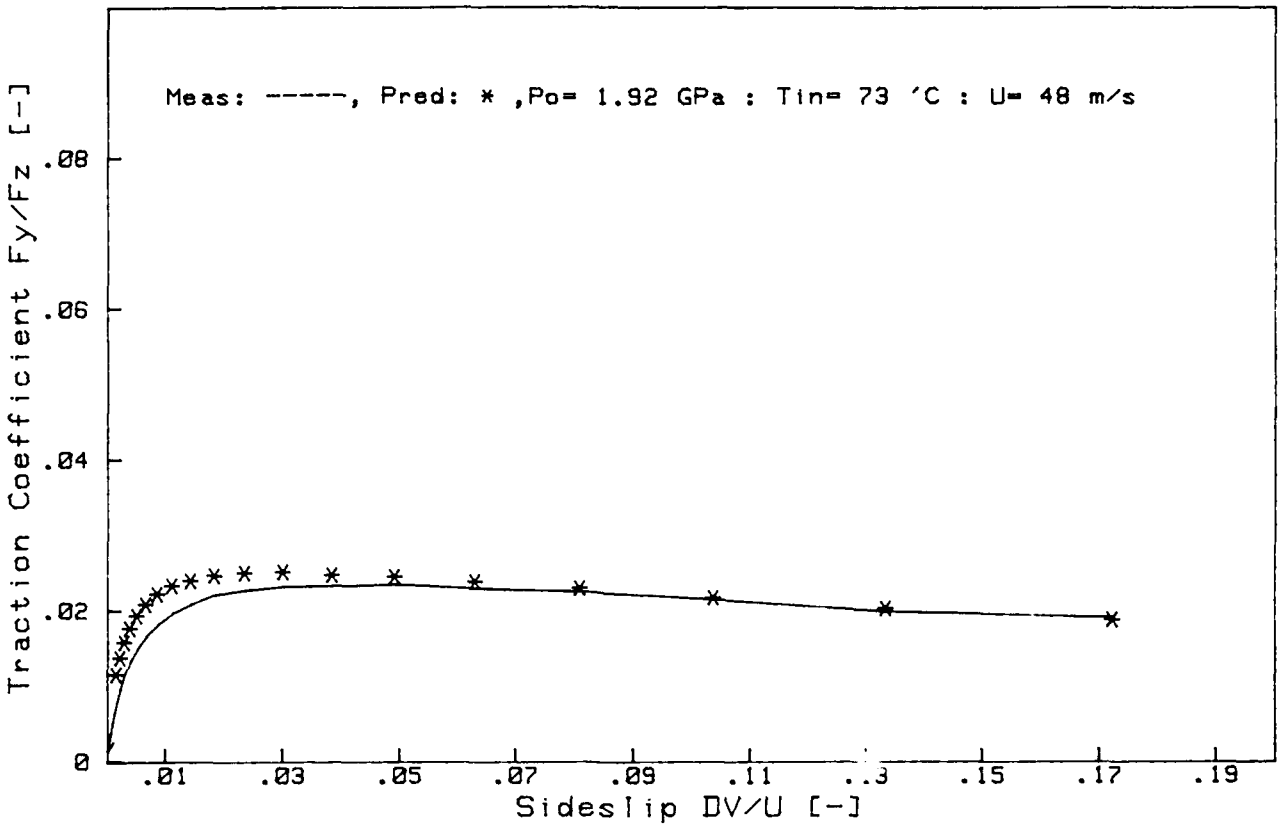
Meas: -----, Pred: * ,Po= 1.92 GPa : Tin= 73 'C : U= 48 m/s
Traction Coefficient Fy/Fz [-]
.08
.06
.04
.02
0
.01
.03
.05
.07
.09
.11
.13
.15
.17
.19
Sideslip DV/U [-]

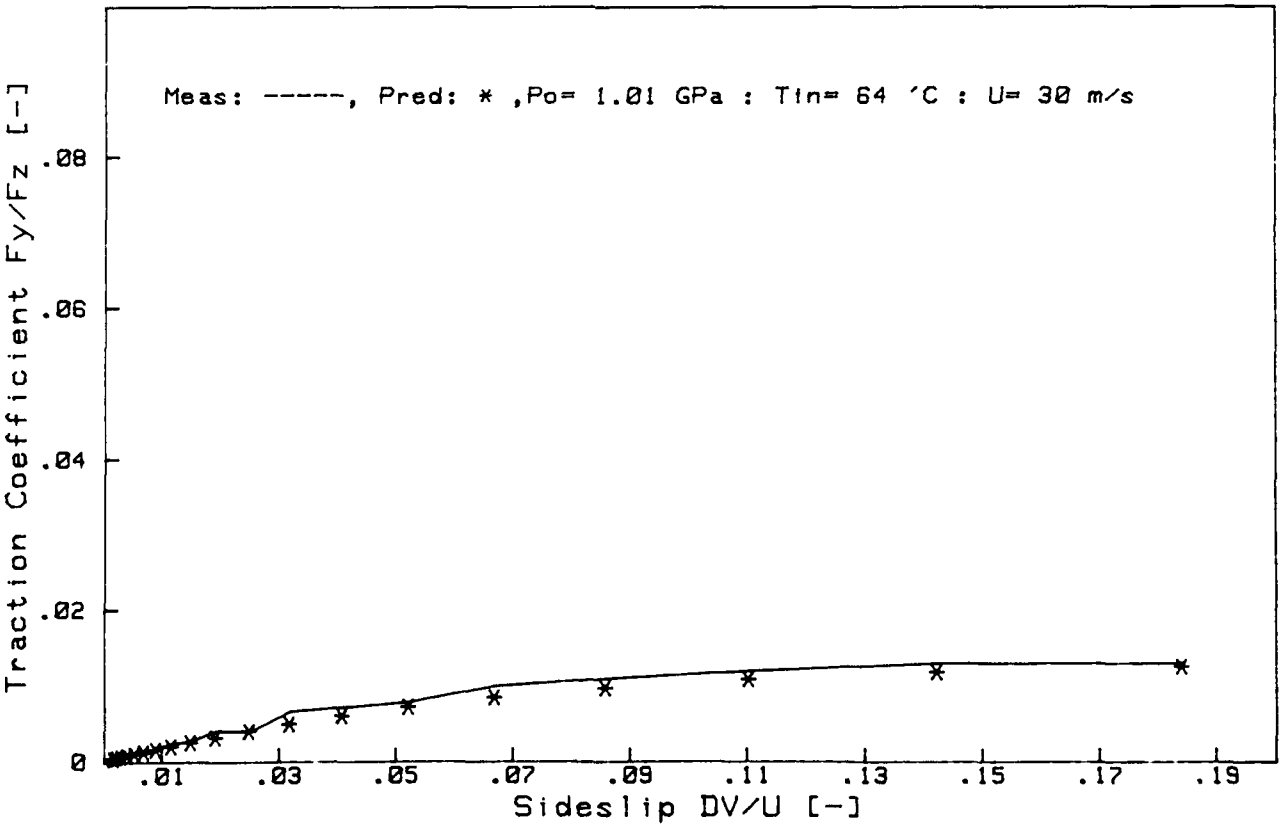
Meas: -----, Pred: * ,Po= 1.01 GPa : Tin= 64 'C : U= 30 m/s
Traction Coefficient Fy/Fz [-]
.08
.06
.04
.02
0
.01
.03
.05
.07
.09
.11
.13
.15
.17
.19
Sideslip DV/U [-]

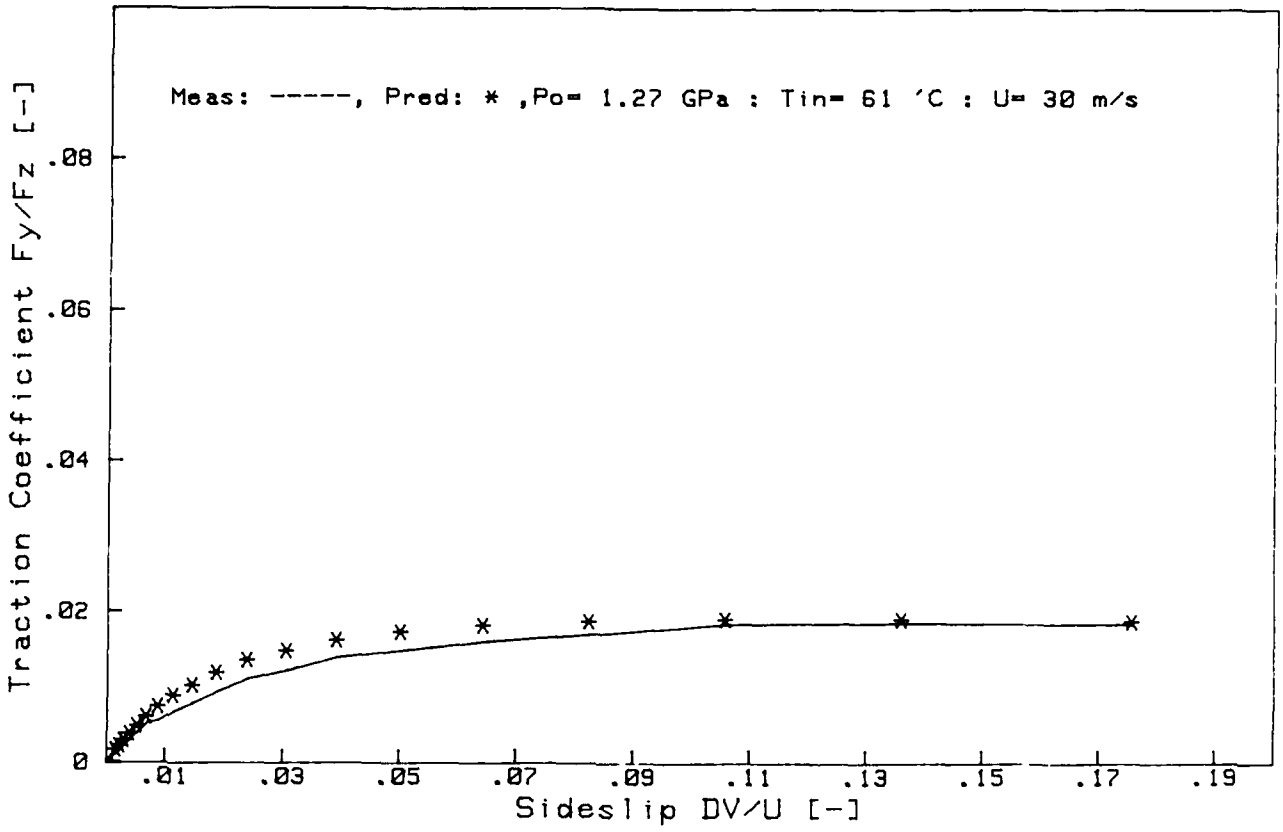
Meas: -----, Pred: * ,Po= 1.27 GPa : Tin= 61 'C : U= 30 m/s
Traction Coefficient Fy/Fz [-]
.08
.06
.04
.02
0
.01
.03
.05
.07
.09
.11
.13
.15
.17
.19
Sideslip DV/U [-]

APPENDIX III

PREDICTED LINE CONTACT DATA

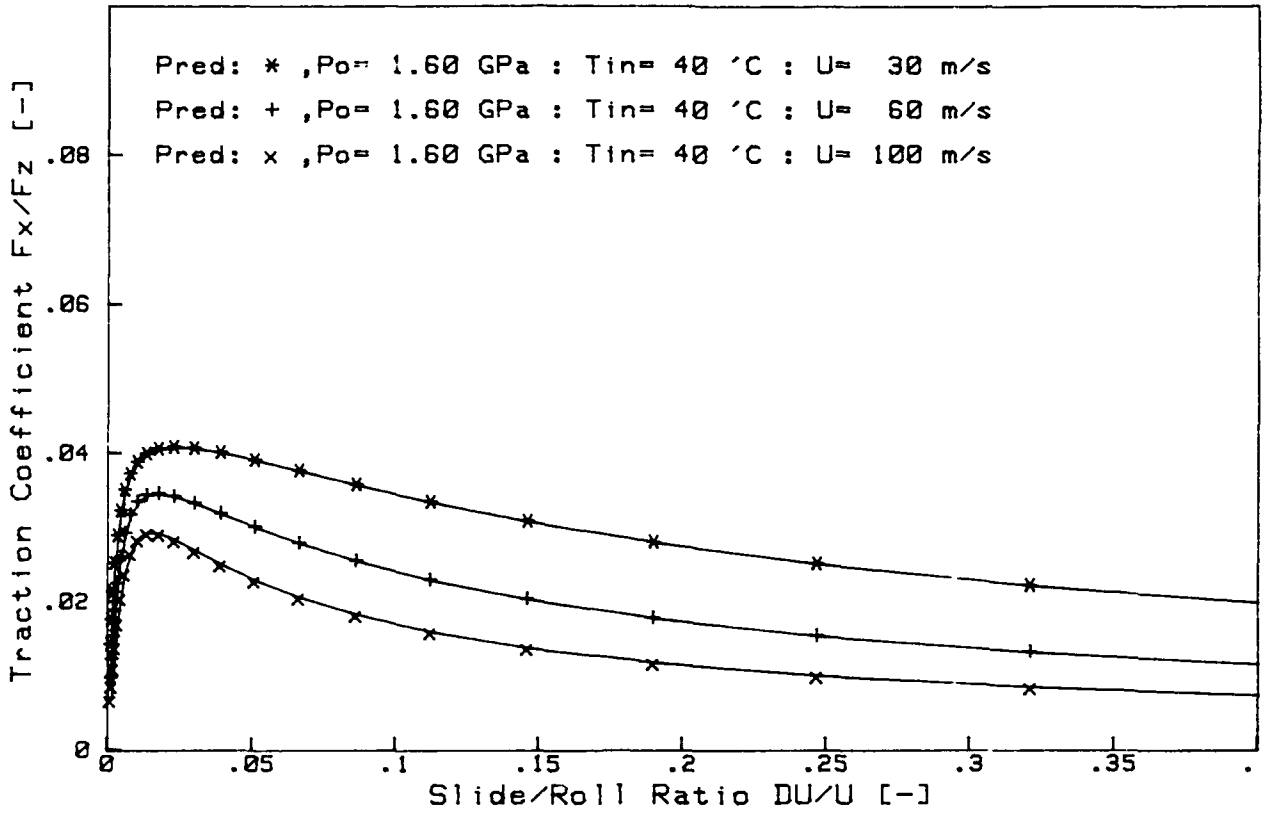
Pred: * ,Po= 1.60 GPa : Tin= 40 'C : U= 30 m/s
Pred: + ,Po= 1.60 GPa : Tin= 40 'C : U= 60 m/s
Pred: x ,Po= 1.60 GPa : Tin= 40 'C : U= 100 m/s
Traction Coefficient Fx/Fz [-]
0
.02
.04
.06
.08
0
.05
.1
.15
.2
.25
.3
.35
Slide/Roll Ratio DU/U [-]

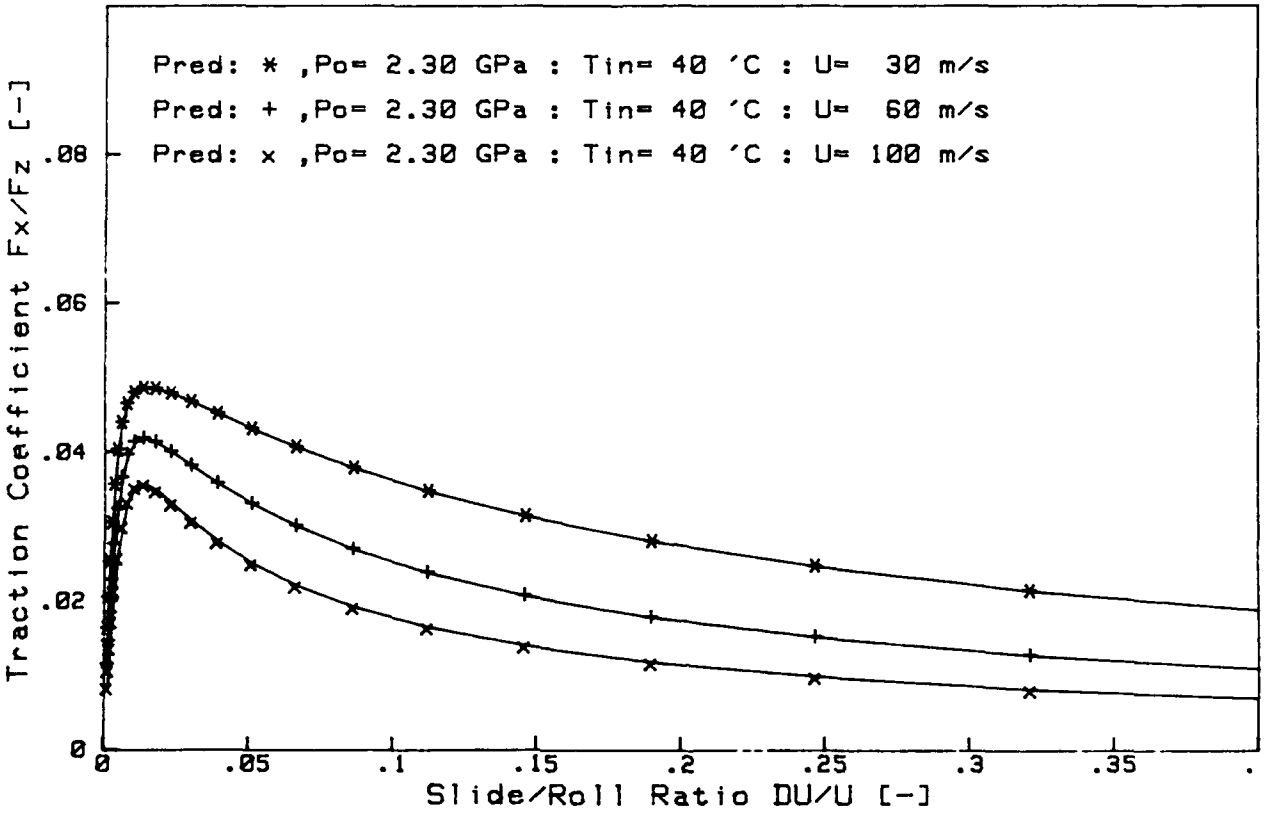
Pred: * ,Po= 2.30 GPa : Tin= 40 'C : U= 30 m/s
Pred: + ,Po= 2.30 GPa : Tin= 40 'C : U= 60 m/s
Pred: x ,Po= 2.30 GPa : Tin= 40 'C : U= 100 m/s
Traction Coefficient Fx/Fz [-]
0
.02
.04
.06
.08
0
.05
.1
.15
.2
.25
.3
.35
Slide/Roll Ratio DU/U [-]

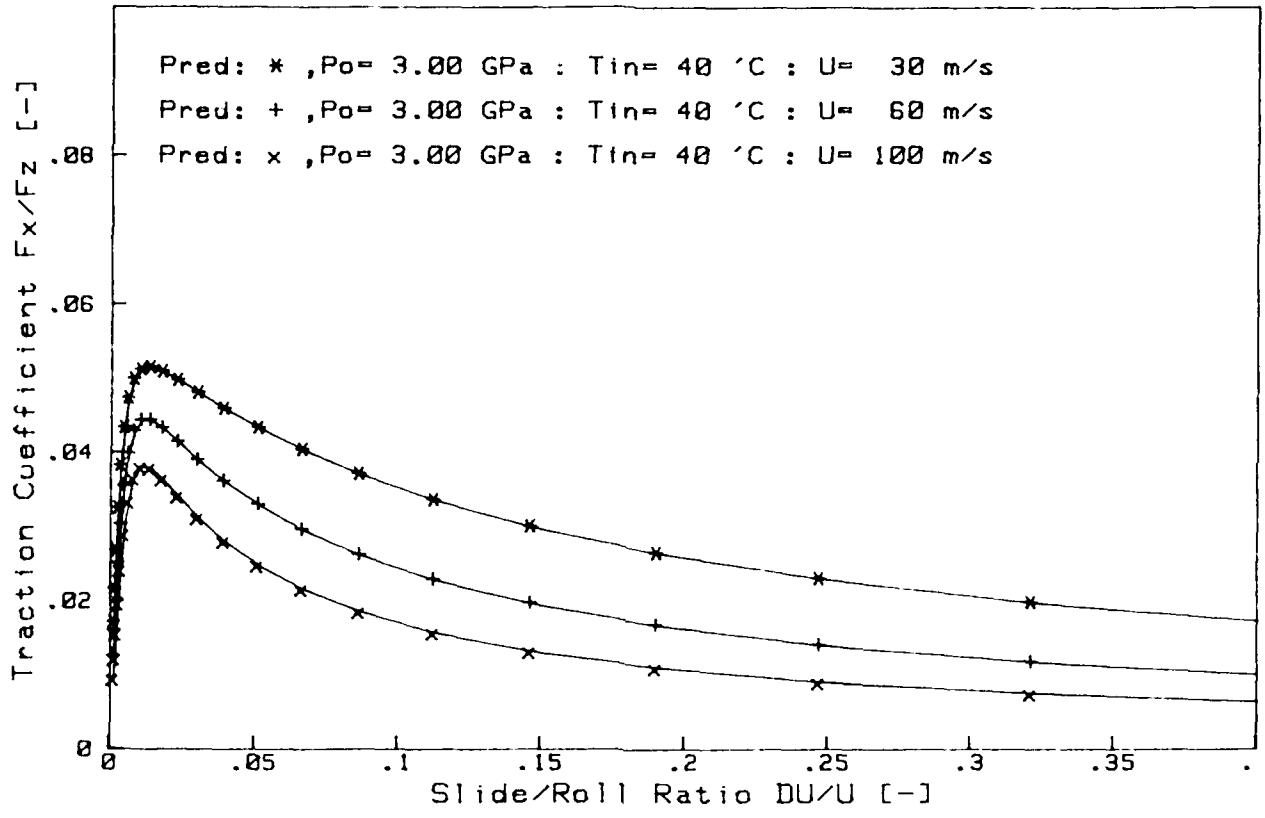
Pred: * ,Po= 3.00 GPa : Tin= 40 'C : U= 30 m/s
Pred: + ,Po= 3.00 GPa : Tin= 40 'C : U= 60 m/s
Pred: x ,Po= 3.00 GPa : Tin= 40 'C : U= 100 m/s
Traction Coefficient Fx/Fz [-]
.08
.06
.04
.02
0
0
.05
.1
.15
.2
.25
.3
.35
Slide/Roll Ratio DU/U [-]

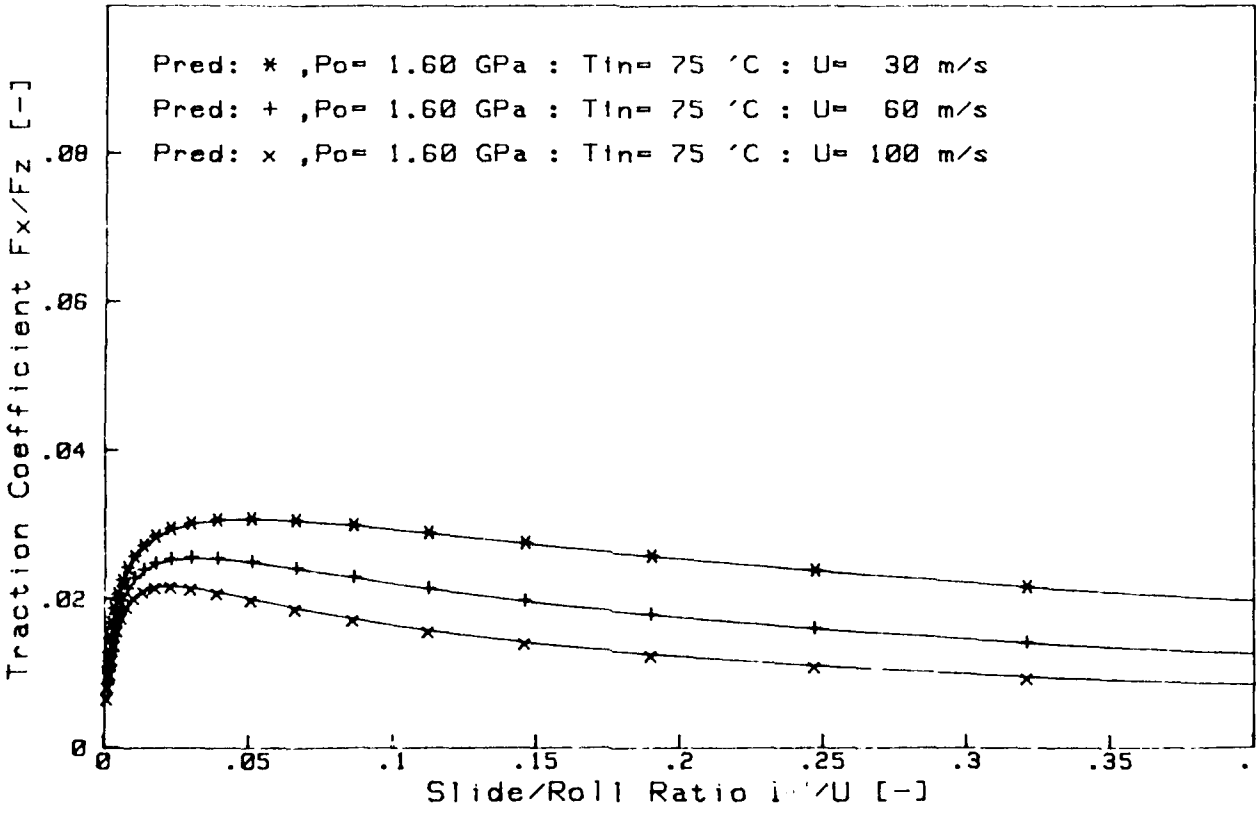
Pred: * ,Po= 1.60 GPa : Tin= 75 'C : U= 30 m/s
Pred: + ,Po= 1.60 GPa : Tin= 75 'C : U= 60 m/s
Pred: x ,Po= 1.60 GPa : Tin= 75 'C : U= 100 m/s
Traction Coefficient Fx/Fz [-]
.08
.06
.04
.02
0
0
.05
.1
.15
.2
.25
.3
.35
Slide/Roll Ratio

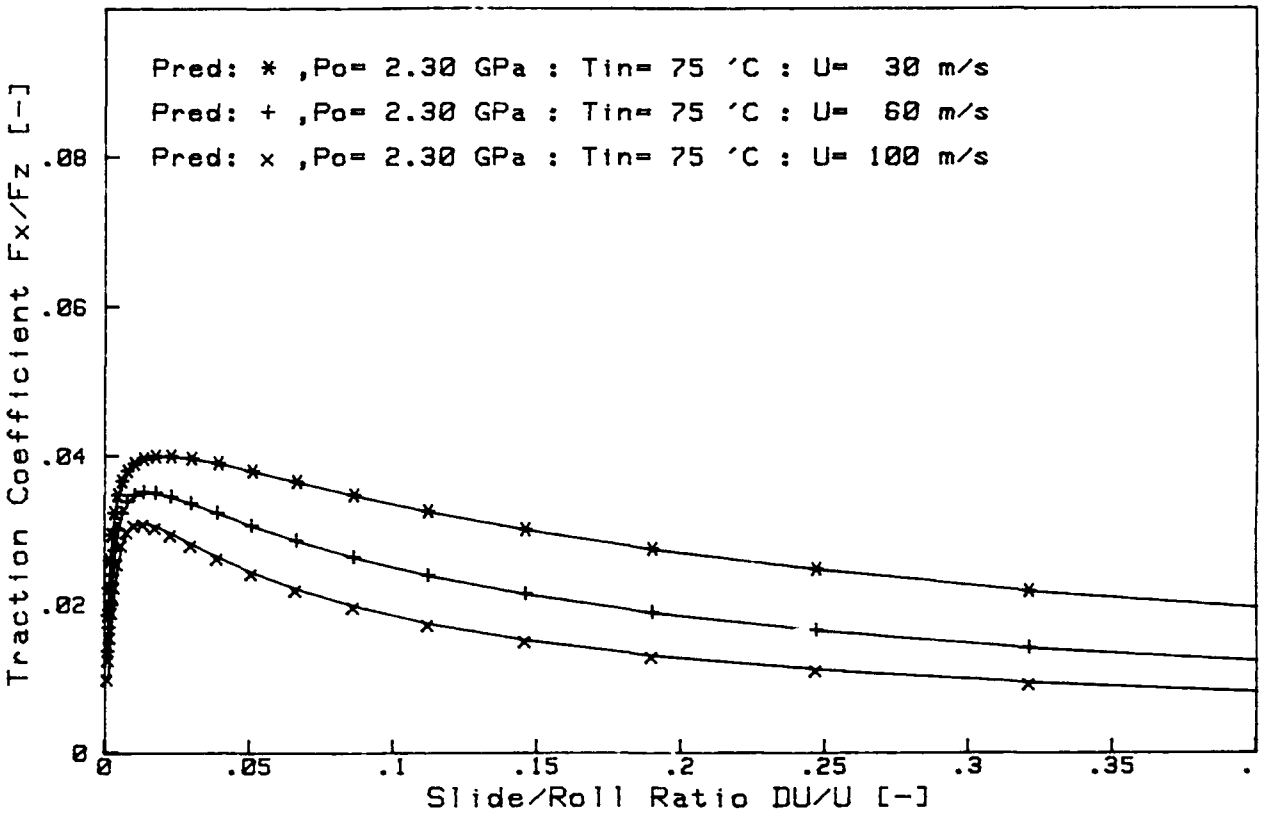
Pred: * ,Po= 2.30 GPa : Tin= 75 'C : U= 30 m/s
Pred: + ,Po= 2.30 GPa : Tin= 75 'C : U= 60 m/s
Pred: x ,Po= 2.30 GPa : Tin= 75 'C : U= 100 m/s
Traction Coefficient Fx/Fz [-]
.08
.06
.04
.02
0
0
.05
.1
.15
.2
.25
.3
.35
Slide/Roll Ratio DU/U [-]

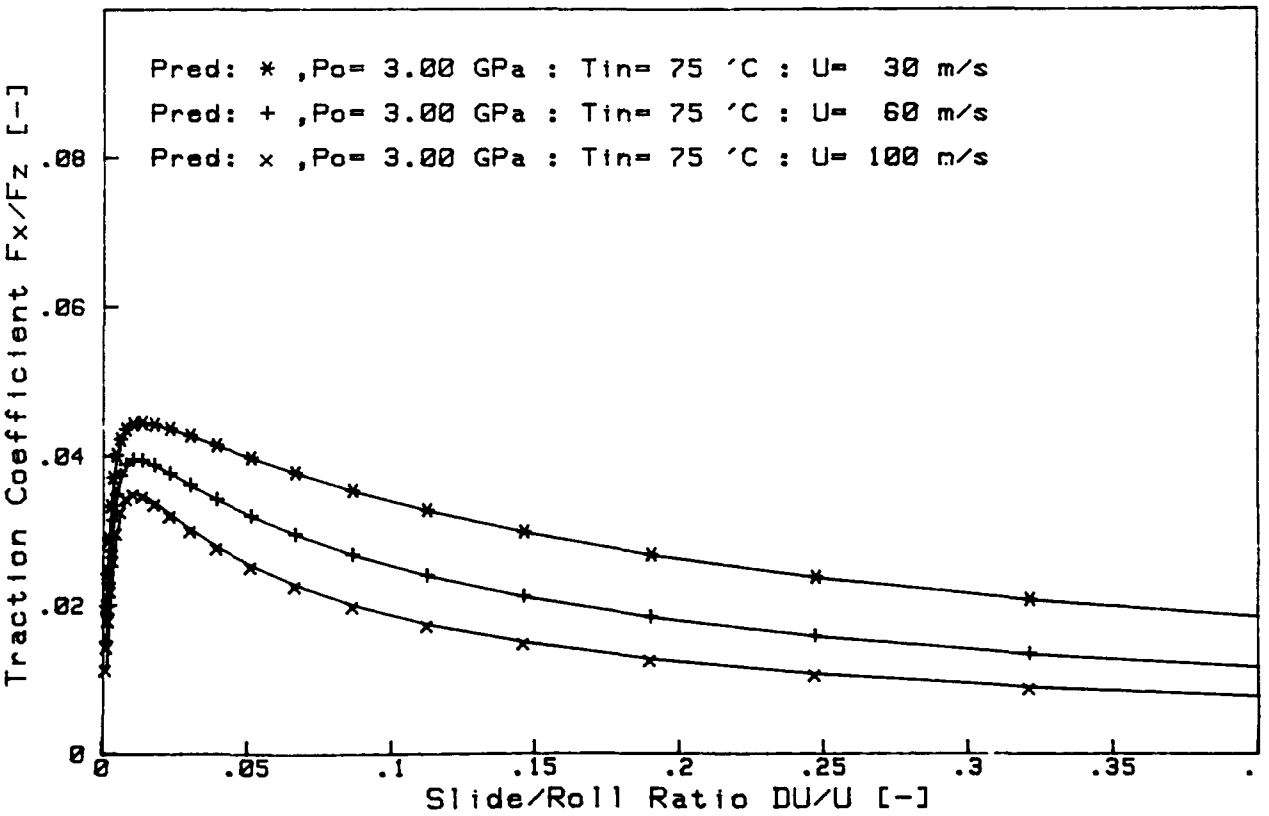
Pred: * ,Po= 3.00 GPa : Tin= 75 'C : U= 30 m/s
Pred: + ,Po= 3.00 GPa : Tin= 75 'C : U= 60 m/s
Pred: x ,Po= 3.00 GPa : Tin= 75 'C : U= 100 m/s
Traction Coefficient Fx/Fz [-]
.08
.06
.04
.02
0
0
.05
.1
.15
.2
.25
.3
.35
Slide/Roll Ratio DU/U [-]

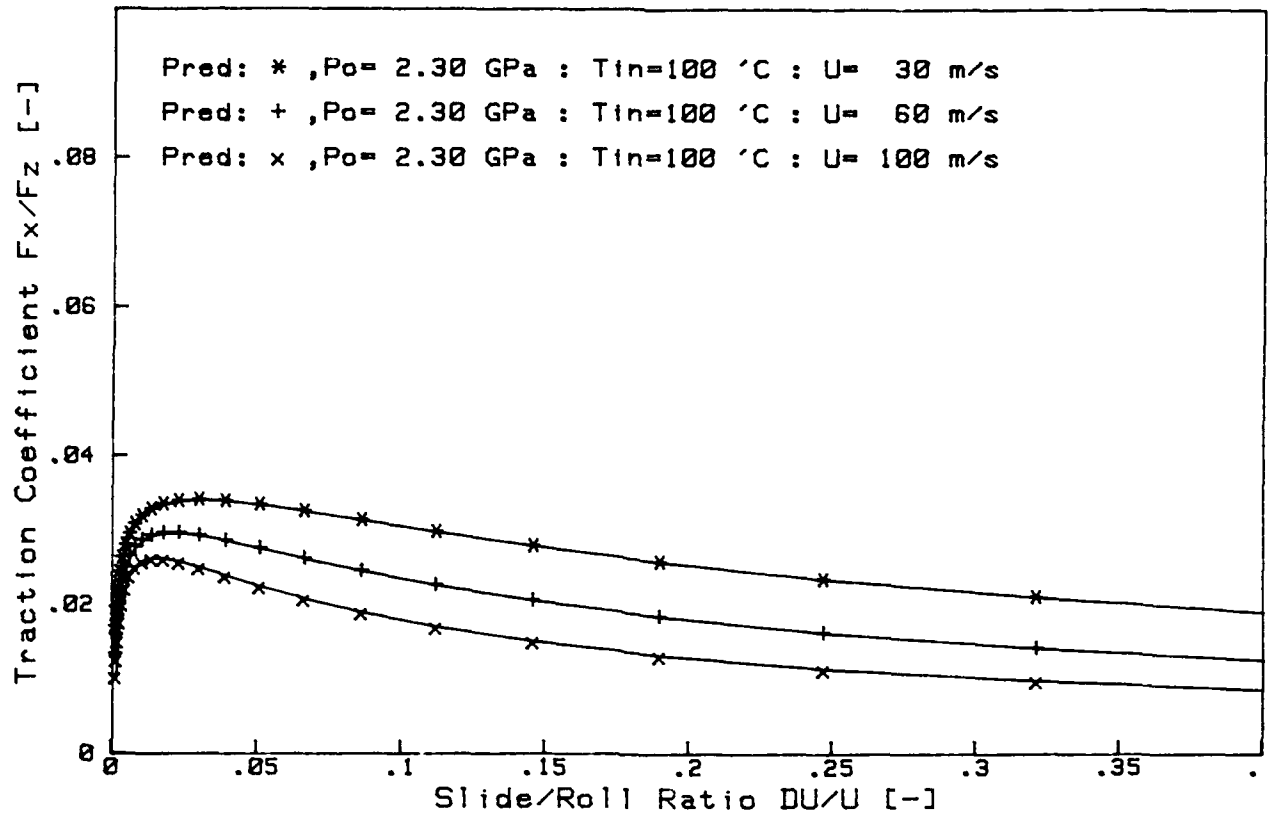
Pred: * ,Po= 2.30 GPa : Tin=100 'C : U= 30 m/s
Pred: + ,Po= 2.30 GPa : Tin=100 'C : U= 60 m/s
Pred: x ,Po= 2.30 GPa : Tin=100 'C : U= 100 m/s
Traction Coefficient Fx/Fz [-]
.08
.06
.04
.02
0
0
.05
.1
.15
.2
.25
.3
.35
Slide/Roll Ratio DU/U [-]

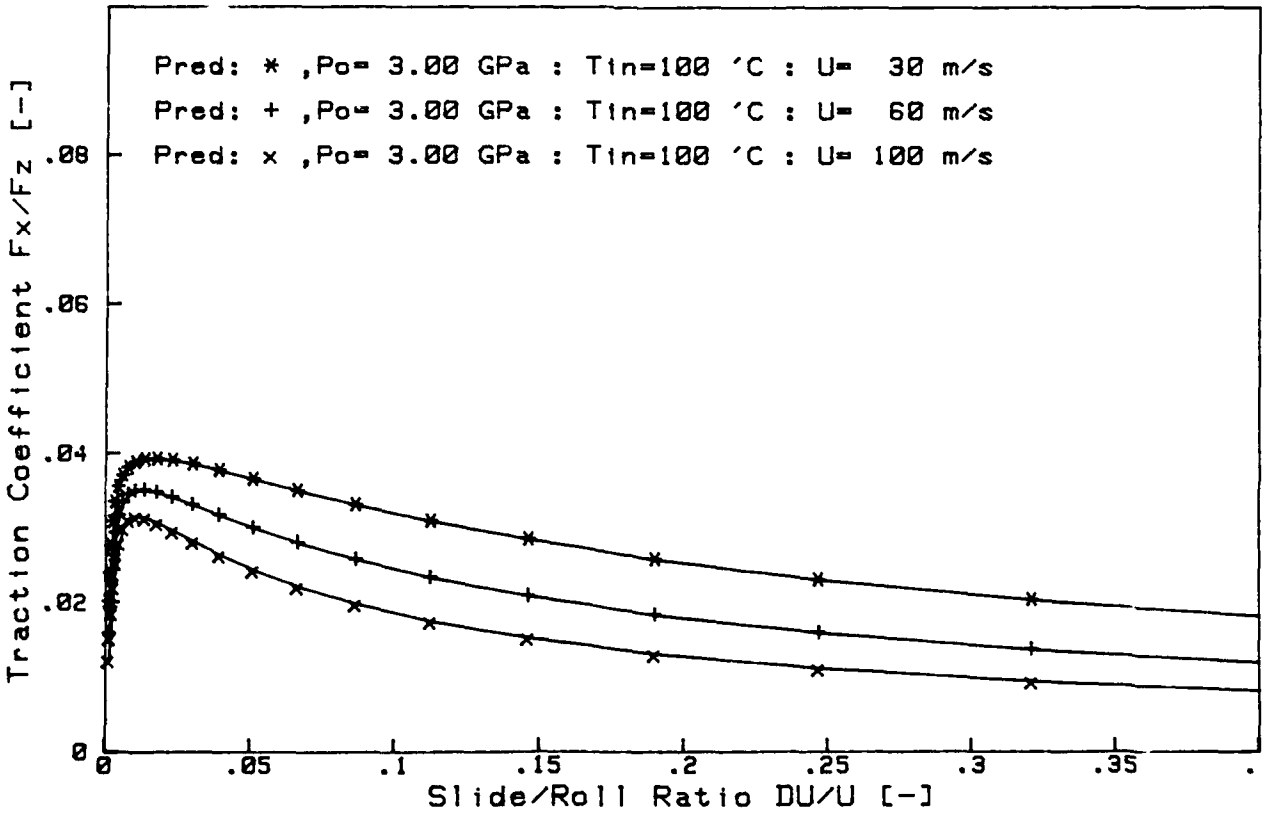
Pred: * ,Po= 3.00 GPa : Tin=100 'C : U= 30 m/s
Pred: + ,Po= 3.00 GPa : Tin=100 'C : U= 60 m/s
Pred: x ,Po= 3.00 GPa : Tin=100 'C : U= 100 m/s
Traction Coefficient Fx/Fz [-]
.08
.06
.04
.02
0
0
.05
.1
.15
.2
.25
.3
.35
Slide/Roll Ratio DU/U [-]

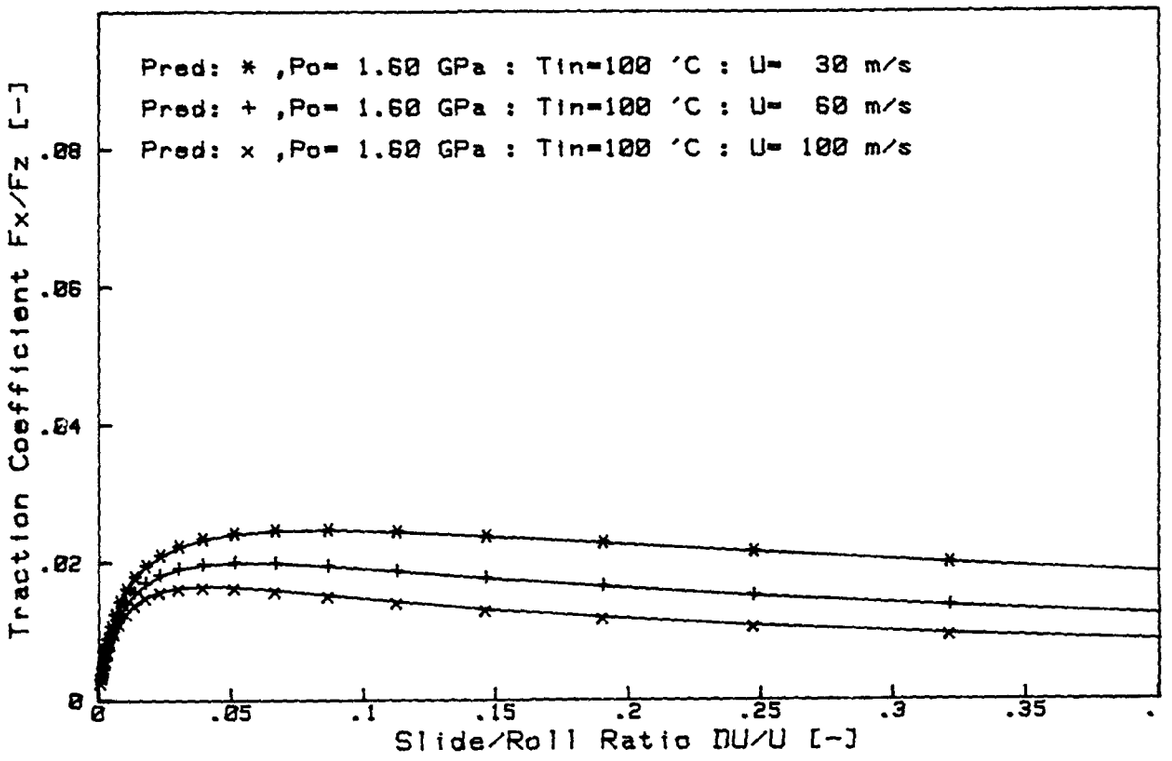
Pred: * ,Po= 1.60 GPa : Tin=100 'C : U= 30 m/s
Pred: + ,Po= 1.60 GPa : Tin=100 'C : U= 60 m/s
Pred: x ,Po= 1.60 GPa : Tin=100 'C : U= 100 m/s
Traction Coefficient Fx/Fz [-]
.08
.06
.04
.02
0
0
.05
.1
.15
.2
.25
.3
.35
Slide/Roll Ratio DU/U [-]